University of Strathclyde

Department of Biomedical Engineering

Design of Locally Actuated Surgical Gripper for Minimal Access Robotic Surgery Applications

Student: Julius Lipskas

Supervisor: Dr. Wei Yao

A thesis presented in fulfilment of the requirements
for the degree of MSc Biomedical Engineering

August 2015

Declaration of Authenticity and Author's Rights

This thesis is the result of the author's original research. It has been composed by the author and has not been previously submitted for examination which has led to the award of a degree.

The copyright of this thesis belongs to the author under the terms of the United Kingdom Copyright Acts as qualified by University of Strathclyde regulation 3.50. Due acknowledgement must always be made of the use of any material contained in, or derived from, in this thesis.

Julius Lipskas

August 2015

Acknowledgements

Firstly foremost, thanks must go to my supervisor, Dr. Wei Yao for his guidance and support throughout this project.

Thanks must also be given to Mr. Justin Caselton for his assistance throughout the project..

Finally, I should thank my family for all of their encouragement and support throughout the year.

Abstract

About 8 million surgical procedures are performed in the UK each year, and 234 million worldwide, and have big influence on healthcare expenditures. It is a invasive health treatment, and therefore large part of these costs are associated with hospital stay, during which patient has to stay under close watch of healthcare professionals.

One of the ways to reduce these costs could be wider application of current and new, even less invasive Minimally Invasive Surgery techniques, such as Single Incision Laparoscopic Surgery and Natural Orifice Transluminal Endoscopic Surgery, what today is potentially limited by lack of suitable instrumentation.

Aim of this project is to develop compact laparoscopic suturing device for robotic suturing applications, based on hybrid, Shape Memory Alloy and DC motor actuation technology. The project will involve development of design specification, device CAD modelling, mechanical and thermal analysis of the design, using Autodesk® engineering software and physical prototype manufacturing.

Table of Contents

List of figures

Equations

List of Tables

1. Introduction

About 8 million surgical procedures are performed in the UK each year, and 234 million worldwide, which have big influence on healthcare expenditures [1]. It is a invasive health treatment, and therefore large part of these costs are associated with hospital stay, during which patient has to stay under close watch of healthcare professionals.

One of the ways to reduce these costs is less invasive surgical intervention. Minimally Invasive Surgery (MIS) has many benefits over traditional open surgery, including better safety, decreased scarring, faster recovery and shorter hospital stay, which result from less traumatic surgical intervention [2].However, these benefits do not come with no cost – today's MIS is more difficult to perform than traditional open surgery and creates high requirements to surgeon's training. Partially, this could be associated with the lack of available advanced surgical tools and instruments.

Application of robotics in surgery was one of the most game changing improvements in recent decade, however, surgical robots are relatively simple in compare with these used in other areas, what, together with lack of tactile and haptic feedback in current systems, makes delicate operations, such as intracorporeal suturing, difficult to perform [3]. However, medical robotics is a promising engineering field, which eventually could let to reduce drawbacks of today's MIS by creating improved surgical tools, based on the recent developments in the field of mechatronics, material science, visualisation and micro actuation technologies. In addition, robotic systems for new surgery techniques, such as Single Incision Laparoscopic Surgery (SILS) and surgery through natural body openings - Surgery and Natural Orifice Transluminal Endoscopic Surgery, potentially could let to perform event less invasive surgical interventions, what in turn could lead into improved healthcare [4].

Motivation

Currently available robotic surgery systems most use actuation sources, that are located outside patients body, power from them is transmitted using mechanical system of slides and cables. However this approach makes system designs bulky, complex, and limits degrees of freedom of the end effector. Placing actuators close to end effectors therefore could let to simplify systems design, reduce mechanism mass and dimensions, what in turn could lead into reduced cost of such systems. In addition, incorporation of sensory elements in surgical gripper design possibly could provide feedback on exerted gripping force and reduce amount of time, required for intracorporeal suturing during surgery.

Aims and objectives

The main aims of this project is to develop the design of compact and locally actuated surgical gripper, suitable to intracorporeal suturing tasks in SILS robotic system, which would be capable to provide feedback about exerted gripping force and test the engineering idea of novel ultra-compact hybrid SMA-DC motor actuator design.

Using requirements, given by SILS system developer and well as design criteria, formulated during literature review, the device was modelled and its performance abilities analysed using Autodesk engineering software. After achieving satisfactory performance in CAD model, the device prototype was manufactured.

2. Literature review

2.1 Minimally invasive surgery

Although laparoscopy was first described more than century ago, minimal invasive surgery at its current form is a relatively new technique, and first truly minimally invasive laparoscopic cholestectomy was performed in 1987.

MIS techniques does not require large incisions, used in traditional open surgery. Instead, it uses one or more relatively small incisions in order to reach internal tissues with specialised tools. Usually these include device with small camera, a laparoscope, and tissue manipulation instruments, such as various graspers, scalpels, and clamps. Special device called trochar is used for invasion through the abdominal wall, and all the tools are inserted through trochar's cannula, which has form of 4-30mm diameter, hollow tube. In order to create and keep space around the surgery site abdominal cavity, pressurised gases are introduced trough trochar, and kept inside due to trochars sealing. Typical MIS instrumentation setup for performing cholecystectomy can be seen in **Figure 1**.

This approach greatly reduces trauma to patients and associated negative effects, such as bleeding, pain, scaring and prolonged hospitalisation. However, it also creates challenging work environment for surgeons: limited visual feedback quality, constricted surgical tools positioning space, tough requirements for tolls size and heavily diminished or completely eliminated tactile feedback. All of these in turn increase surgery time, creates a need for expensive and sophisticated instruments and require highly skilled professional to perform [2].

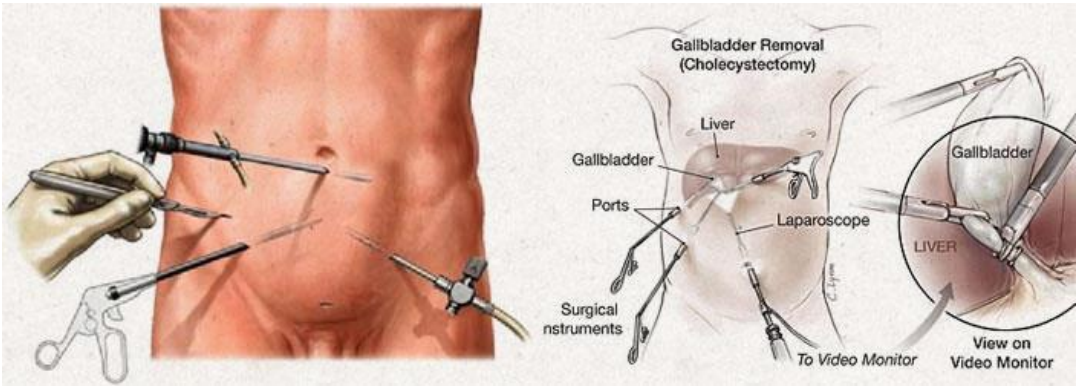

Figure 1. Typical surgical instrumentation setup for Minimally Invasive Colystectomy [5]

2.2 Robotic systems for Minimally Invasive Surgery

Robotic surgical assistance systems were introduced as an attempt to overcome visualization and dexterity issues in conventional MIS.

The was the first minimally invasive robotic assisted surgery was performed in 1991, using device called “Probot”, developed in United Kingdom, and was used in prostate surgery [6].

There is two commercially available MIS robotic systems currently on the marked.

The daVinci® (Intuitive Surgical, Sunnyvale, CA) system is a more advanced robotic system, which enables a surgeon to control robotic arms with attached surgical instruments from remote control unit. Patient side cart is controlled from surgeon’s console, which provides comfortable workplace with 3D visualisation of surgical site and translates surgeon’s movements from finger grasps to patient side cart. Endowrist® robotic instruments, used in this system, are capable to provide seven degrees of motion and are actuated with the help of tendon mechanisms, which in turn are connected to actuators, placed outside patients body. During surgery, these instruments can be interchanged using quick release mechanisms. They are

8mm in diameter. The daVinci® also has a visualisation system, which consists of 3D endoscope, image processing and visualisation equipment, and is responsible for providing visualisation for surgery room team [7].

Zeus robotic surgical system was approved by FDA in 2001 and is produced by Computer motion inc., was designed for MIS microsurgery procedures, such as coronary artery bypass grafting and beating heart surgery. It consists of three robotic arms, one of which is used for endoscope placement and manipulation, while remaining two serve as manipulators, to which interchangeable surgical instruments are attached. Its robotic arms are controlled and surgical suite visualised with the help of surgeon's console, that provides high definition 2D or 3D view also scales and filters surgeons hand movements exerted on control levers, in order to provide more precise control. Surgical instruments, used in this system are 5mm or less in diameter and are capable to provide 5 DOF motion at the instrument tip. They are actuated with the help of electric motors, located outside patient's body [8].

Although there are approximately 3400 [7] daVinci® system and 50 Zeus system units [8] in surgery rooms worldwide, wide use of the them remains limited due to large size, high cost, and the diminished impact of the dexterous improvements for performing less complex surgical procedures.

2.3 Minimal Access Surgery

Surgical procedures based on minimally invasive techniques are well established, and are commonly used for many routinely performed surgical interventions, however, new modalities of MIS attempts to further reduce to patients trauma and associated healthcare sector expenses.

Complete elimination of external incisions would be a significant step towards reducing the invasiveness of surgical procedures. Natural orifice transluminal

endoscopic surgery (NOTES)is new experimental surgical technique, which might eventually achieve this target. Its main concept is to use natural orifice, such as mouth, urethra, and anus, in order to reach required surgery suite. First natural orifice procedures dates back to 1940, when culdoscopies were performed using an endoscope, passed through recto-uterine pouch in order to inspect organs in pelvic cavity. The first report of true NOTES in canine was published in 2004, and followed by announcement of first transgastric appendectomy, performed using natural orifice transluminal endoscopy in male patient. Theoretically, the elimination of external incisions could potentially have many advantages over laparoscopic and traditional open surgery techniques, including complete elimination of skin and abdominal wall wounds, less trauma to patient, could let to avoid wound infections, further reduce pain, and improve cosmetics and recovery times. In addition, this kind of surgery could suitable for certain groups of patients (for example, obese patients), where application of traditional surgeries could be complicated or even impossible [9].

However, current NOTES techniques have many complicated aspects too, including concerns about potential intra-abdominal infections, lack of approved surgical techniques, instrumentation and training.

While NOTES can be the ultimate target of minimally invasive surgery, significant surgical and technological challenges creates interest in less complicated its modality, a Single Incision Laparoscopic Surgery (SILS), which could also be an important step towards solving issues with NOTES.

SILS, which uses most commonly uses single incision in the umbilical region, is not a new technique, and had been around for more than 30 years, with first techniques, applied in gynaecological surgery, reported in late and followed by reports of performed of advanced pelvic extirpative surgery and appendicectomies in 1992. As it uses single incision instead of multiple ports in conventional MIS, it can offer better cosmetic outcome, reduced pain and risk of complications due to port site infections and hernias [10].

Accessing the peritoneal cavity through a natural orifice or a single abdominal incision can be preferred by many patients. However, using today's surgery techniques and tools, both methods can be complicated. It can be difficult to have multiple instruments inserted through a natural orifice or an incision and simultaneously provide required manipulation and visualization capabilities. In addition, current endoscopic and laparoscopic instrumentation was not designed for NOTES and SILS procedures, and new technologies that can overcome these challenges and provide the surgeon with adequate visual feedback and triangulation are necessary.

A design concept of modular robotic surgical system manipulator for SILS and NOTES applications, which potentially could overcome issues with dexterity, visualisation, surgical tools mobility and triangulation of current robotic surgical systems, can be found in Wey Yao and Peter RN Child work [11]. Proposed surgical system consists of steerable visualisation unit, two surgical grippers, which are attached to annular platform, in addition, extra tools could be inserted through hollow shaft of endoscope. These modules together should ensure good triangulation capabilities. This assembly in turn is connected to Stewart Platform, which should provide required orientation for system tools. Their system could be inserted through natural orifice or single incision in folded state and expanded when it reaches required surgery place. After surgery, device could be folded again and removed from patient body.

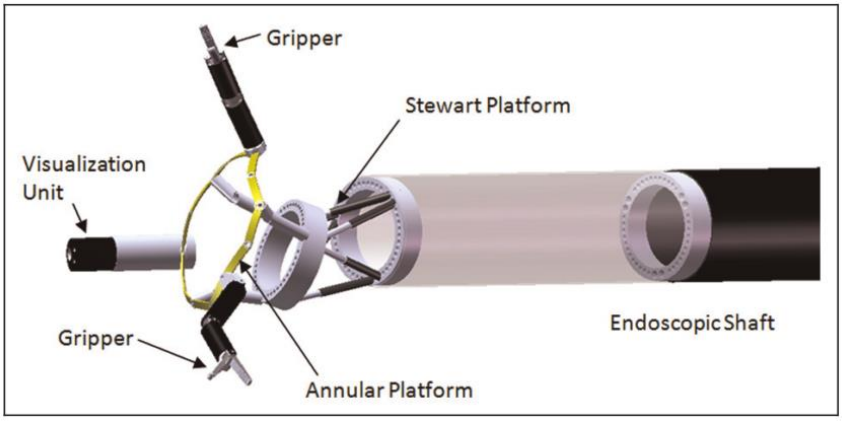

Figure 2. Robotic system design for minimal access surgery [11].

2.4 Conventional Laparoscopic Suturing and Knot Tying Process

Intracorporeal suturing and knot tying is oldest and most common suturing technique in MIS, which is used to connect tissue layers after injury or surgery. It is performed with a suturing needle and two elongated needle drivers which are used to hold the tissue and drive the needle with suturing thread (**Figure 3**). Tools are inserted through inserted through the laparoscopic trochars. Suture placement is performed manually inside body.

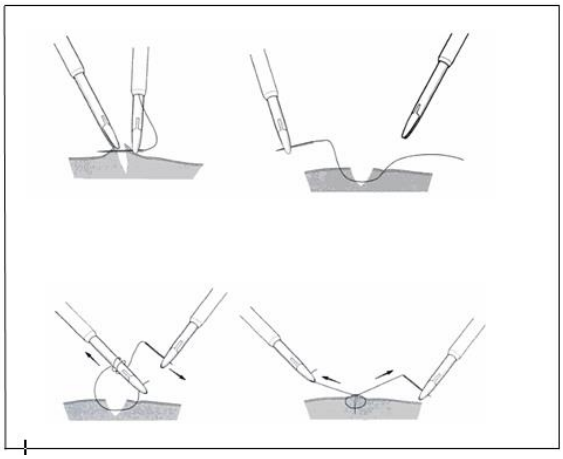

Figure 3. Conventional suturing and knot tying technique [12]

The great variety of tools, materials and methods are used in today's MIS intracorporeal suturing, however most commonly it is performed using curved needles, bio-absorbable suturing threads, and interrupted sutures [13]. Examples of common suturing techniques can be seen in **Figure 4**.

The main function of surgical gripper during suturing is common for most of them: it is either used to hold the tissue in place to provide more stability, or to hold and drive the needle with suturing thread. Therefore, most important features of surgical gripper should be appropriate holding force, stability, ability to provide appropriate spatial orientation and manipulation force. In addition, several requirements arise from invasive surgery nature and restricted operating space, such as excellent biocompatibility and restrictions to tool size.

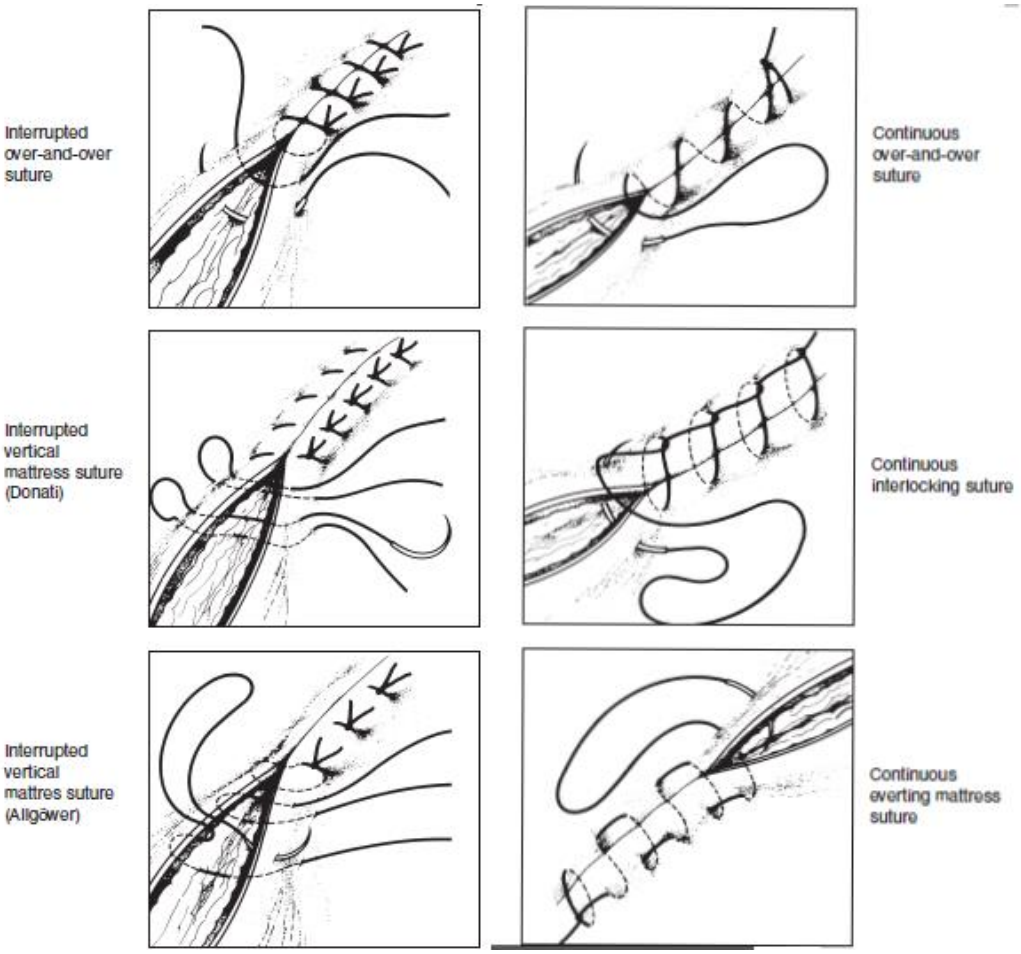

Figure 4. Common suturing techniques [14]

2.5 Haptic and tactile feedback importance

Intracorponeal suturing is one of the most difficult tasks to perform and takes significant amount if surgery time. It is even more complicated in robotic surgery – it's tools are mechanically decoupled from surgeons hands, therefore tactile and haptic feedback is completely eliminated, and visual feedback remains the only solution to get an impression of the forces applied. However, because the deformation of tissue can be specific for each patient, it can result in insufficient quality of sutures and knot. In addition, current robotic systems do not provide feedback on gripping forces, what can result to unintentional tissue damage [15].

2.6 2.4 Sterilisation of surgical tools

Sterilization of medical devices, surgical instruments and equipment is critical a critical aspect of the modern health care delivery system and has high impact on patient and healthcare personal safety.

Reusable surgery tools require proper decontamination after each use. It is achieved physical and/or chemical treatment process, during which potentially harmful biological and chemical materials residues and pathogens are removed from surgical tool by means of mechanical cleaning, aggressive chemical environment and/or heat.

Mechanical cleaning is often performed using around 18kHz ultrasound in neutral solution bath, during which bulk of contaminants is removed. It is followed by sterilisation treatment. The most common sterilizing agents used in healthcare facilities today are ethylene oxide gas, hydrogen peroxide gas plasma, liquid chemicals, ozone and saturated steam. Summary of main sterilisation parameters can be seen in **Table 1**[16].

Sterilisation treatment	Ethylene oxide gas	Hydrogen peroxide gas plasma	Liquid chemicals	Ozone	Saturated steam
Temperature, $°C$	30-62	40-55	50	30-34	121-132
Exposure Time, min	120	28-75	12-600	270	4-30
Sterilisation mechanism	Alkylation	Aggressive chemical environment	Aggressive chemical environment	Aggressive chemical environment	Heat

Table 1. Environmental conditions during sterilisation

2.7 Actuation in surgical robots

As it was revelled above, currently available surgical robots mainly use linkage and tendons mechanisms connected to actuators, located outside patients body, in order to provide required forces for end effectors. This approach has several drawbacks, including relatively complex and bulky designs, increased dimensions and restrictions to tools mobility [17].

An attempt to solve these issues could be surgical-operation-by-wire (SOBW) concept, main idea of which is to place actuation source as close possible to end effectors, and only provide driving signals and various forms of activation energy. However, development of device using this concept requires to use extremely compact actuator with high power density. Micro actuators are constantly improved and tending to get smaller, lighter and more efficient, however, there still is very little choice of suitable micro actuators, which could be used in such designs, as in addition to size and power density limitations, medical robotics also have high requirements for device and activation energy safety and biocompatibility.

The most convenient for such applications must be electrically activated actuators, as they use relatively safe and convenient form of activation energy and control in form of electric currents. Comparison of most common electric actuators in terms of power density, strain, speed and activation energy and suitability for custom designs is shown in **Table 2** [18], from which is evident, that shape memory alloy based actuators can provide highest power density, acceptable strain output and therefore most compact designs. In addition, they are easy to manufacture, reliable, can be easy applied in custom designs, and are widely available.

Actator type	Strain, %	Pressure, MPa	Energy density, J/cm3	Realitive speed
Electroactive polymer	63-215	3-7.2	0.75-3.4	Medium
Electromagnetic (voice coil)	50	0.10	0.025	Fast
Piezoelectric	0.1-1.7	4.8-110	0.0024-0.10	Fast
Shape memory alloy	>5	160-200	>100	Slow
Thermal expansion	1	78	0.4	Slow
Magnetostrictive	0.2	70		Medium

Table 2. Comparison of common actuation technologies

2.8 Shape memory alloy (SMA) based actuation

SMA based actuators provide force and displacement output due to shape memory phenomenon associated with material solid state phase change from martensite to austenite when material I heated to above its characteristic phase change temperature. Solid state phase changes in these alloys take place over relatively

narrow range of temperatures (30-50°C), however it gives large changes in material modulus, and in turn to SMA element`s shape recovery to its original.

Typical phase change curve, with evident temperature hysteresis is shown in **Figure 5**. 1. Below full martensite temperature (M_F), SMA element consists completely from detwinned martensite, which has significantly lower elastic modulus than austenite, and element is easy to deform. During heating, element reaches austenite start temperature (A_S), and if element was deformed it begins recovery of its original shape, which is completed at full austenite temperature (A_F), where element consist entirely form austenite. During cooling, temperature hysteresis is evident, and material has to reach approximately 30°C lover temperature than (A_F), from where its starts to change atomic structure back to martensite [19].

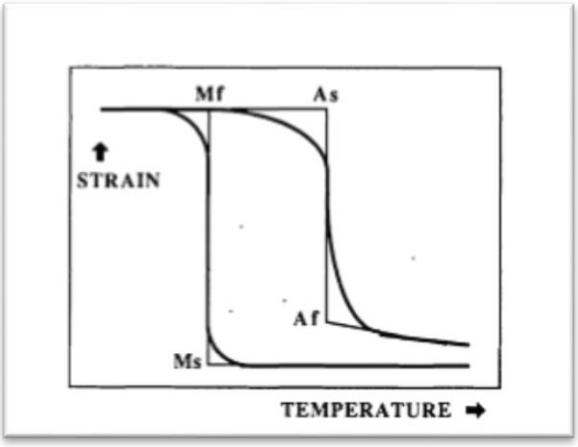

Figure 5. Typical SMA phase change curve

The response speed of SMA actuators depends on heating/cooling speeds, and while heating, which is usually achieved due to Joule effect using electric current, can be very fast, cooling speeds in general are much slower, and leads to reported typical full cycle frequencies of SMA actuators of 0.1-0.5Hz [20][21][22].

Actuators usually consist of SMA element and bias element, which is used to provide force, required to deform SMA element from its austenite shape.

Characteristic activation temperatures SMA are dependant from alloy composition and can be altered by changing proportions of metal in alloy. They also follow Clausius–Clapeyron relation, and therefore are higher if material is subjected to stress. In addition, repetitive of heating/cooling cycles can lead in further response un-linearity's which makes accurate open-loop control complicated.

SMA elements design methods of can be found in literature [19].

Reported efficiency of SMA actuators is about 5%, and as other energy is released as a heat, application of this type of actuators in MIS surgical instruments potentially could cause heat-associated problems.

2.9 Hybrid actuator

Another way to obtain required actuation forces and displacements could be combination of two actuators of different kinds, or hybrid actuator.

In suturing gripper, bulk of actuators displacement is used for opening and closing the jaws, and should not need maximum force output, which is only required to provide appropriate gripping and holding force, when the gripper is in closed position. Therefore, low force, large displacement element could be used for bulk of motion, while high force element could be activated only when large force output is needed. Particularly suitable looks combination of electric DC motor and SMA element, as it potentially could let overcome issues with SMA alloy actuator inefficiency and low operating frequency, and would let to use much smaller DC motor.

Chowdhary K. et al. [17] report design of hybrid SMA and electric DC motor actuator for MIS applications. They have used a metric screw to convert rotation into required 1mm of linear motion, and connected in series SMA wire element to produce required maximal force output of 24N. However, in their design SMA

element should remain active during all period of time when maximal force output is needed, and therefore would not eliminate actuator overheating issues. In addition, relatively big length of such actuator (40mm) would increase load on robotic arm spherical joint.

3. Design Methodology

The Analysis-Synthesis-Evaluation model was used in this work in order to produce device design. Design process involved considerable amount of analysis, production of design decisions and experimental verification of design suitability. in order to simplify the design process, design process was split in two parts: gripper design and actuator design. In addition, this approach potentially could let to produce modular device design. Design process flow chart is shown in image 15.

Analysis stage was used to produce required design specification, based on given dimensional and device control requirements and literature review findings.

During synthesis stage, several possible design concepts were developed and evaluated in terms of suitability. Based on evaluation results, best concept was chosen.

In the evaluation stage, the chosen design solution was modelled using CAD software and necessary improvements were made. Finally, physical prototype was manufactured and its testing attempted.

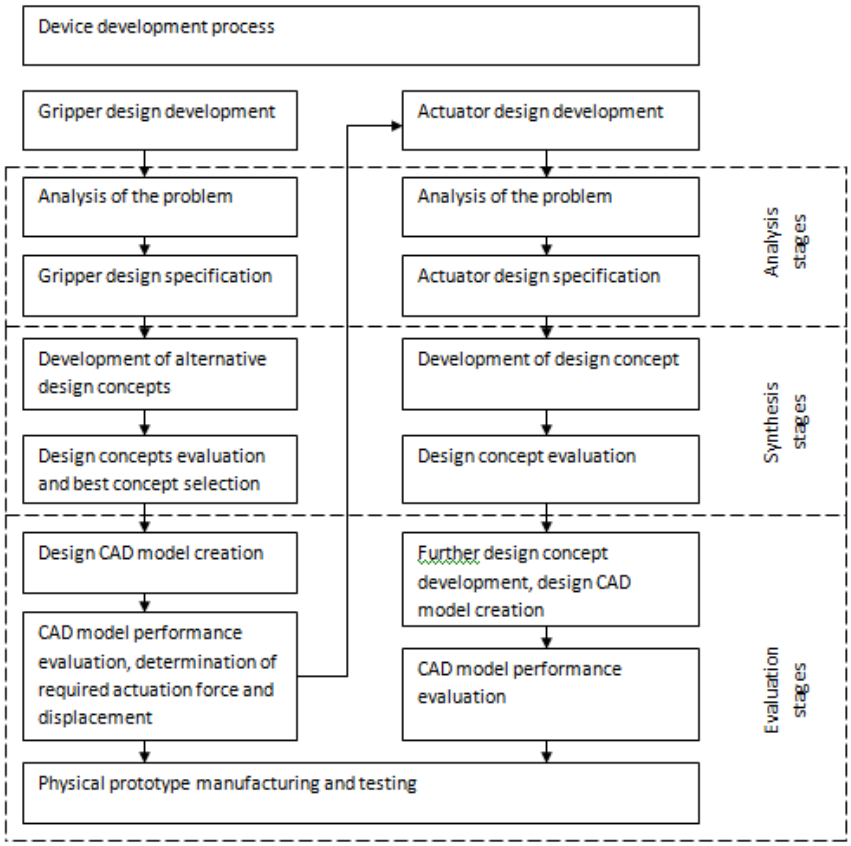

Figure 6. Design process flow chart

3.1 Gripper design

3.1.1 Analysis stage

3.1.1.1 Material choice

Surgical instruments should be made from robust and biocompatible materials, as it should poison patient`s organism and withstand contact with blood, body fluids and tissue, which are very corrosive and potentially could lead to the degradation of the surgical device if it is made from inappropriate materials. Stainless steel is commonly used in surgical instruments production. It has good biocompatibility properties and therefore could be material of choice. In addition, it has good mechanical strength properties, and therefore some dimensions of gripper parts could be minimised and still withstand appropriate loads. The most common in medical devices are Austenitic 316,and Martensitic 440 stainless steels, also often called as “Surgical grade stainless steels”.

3.1.1.2 Gripping force

In order to function properly, gripper must hold tissue or suturing needle with appropriate force. The main factors, influencing this function is gripping force, jaws surface texture and coefficient of friction between the grasper jaws and work object surfaces. Most important of which must be the griping force. Reported values of griping forces, provided by surgical tools, range from 1 to 20N. Summary of reported values is given in **Table 3**.

Study Author	Berguer R.et al., [23]	Westebring-Van Der P et al. [24]	Mucksavage, P et al. [25]
Range of gripping forces, N	0.7-4.2	1.2-8	2-20
Average grabbing force, N			6N

Table 3. Summary of gripping force values

Most of currently available graspers have grooved surface texture on their jaws, function of which should be to increase surface area or deform gripped object in order to increase holding force. However influence of different textures out of the scope of this work, which will only focus on gripping force.

3.1.1.3 Device dimensions

Surgical gripper, which will be designed during this work, is intended to be used in SILS robotic system, which is currently being developed by University of Strathclyde PhD student Justin Castelton, and therefore dimension requirements except device length were given. Device will serve as an end-effector and will be attached to a robotic arm, shown in **Figure 7**. The length of the device will have big influence on joint 2, and therefore should be kept as short as possible.

3.1.1.4 Design specification

Diameter - should not exceed 12mm

Length - as short as possible

Jaws opening - 10mm at the tip of jaws

Opening angle - 60 degrees

Material - stainless steel 316

Device should withstand loads, required to produce 6N gripping force at the tips of the jaws

3.1.2 Synthesis stage

3.1.2.1 Design alternatives

Number of various could be used in order to achieve required design parameters. Main criteria, which could be used to choose most suitable one are overall length of mechanism. Another important criterion arises from need of actuation, as inappropriate design could create unnecessary need for high actuation forces or moments. In addition, the ease of manufacturing could potentially have influence of device price, and therefore also should be evaluated. Kinematic schematics of potential mechanisms of choice are shown in table 11, together with simple analysis of suitability. Points system was used for suitability evaluation. For suitability evaluation purposes each mechanism was ranked in length, actuation force, and ease of manufacturing category. In order to give weight for each category, multipliers of 1, 2 and 3 were used.

Schematic view of the mechanism	Length	Actuator load	Ease of manufacture	Sum of points
Worm gear				
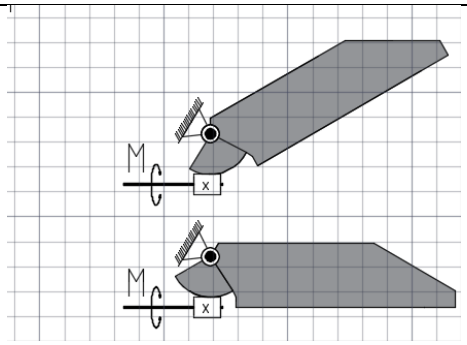	6	2	1	9
Linkage				
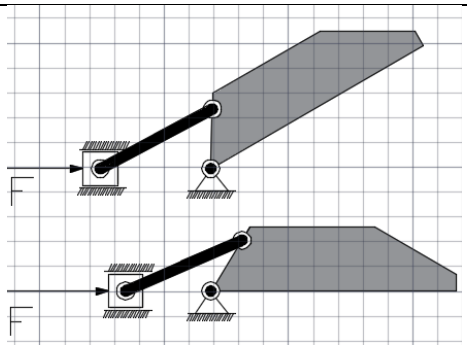	3	4	3	10
Sliding slot and block				
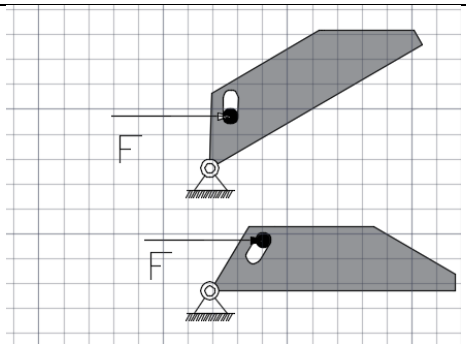	9	4	2	15

Table 5. Gripper mechanisms suitability evaluation

Based on analysis results, sliding slot mechanism was chosen as a base for design. Traditional gripers often have sliding slot mechanism opposite to the jaws, however in order to keep the mechanism as short as possible, sliding mechanism could be incorporated in front part of the jaws. In addition, screw mechanism, for conversion

of rotation of DC motor into linear motion also could be incorporated into grippers length, and therefore further shorten the device.

3.1.3 Evaluation stage

In order to test design suitability, griper was modelled using Autodesk Inventor software (Figure) .

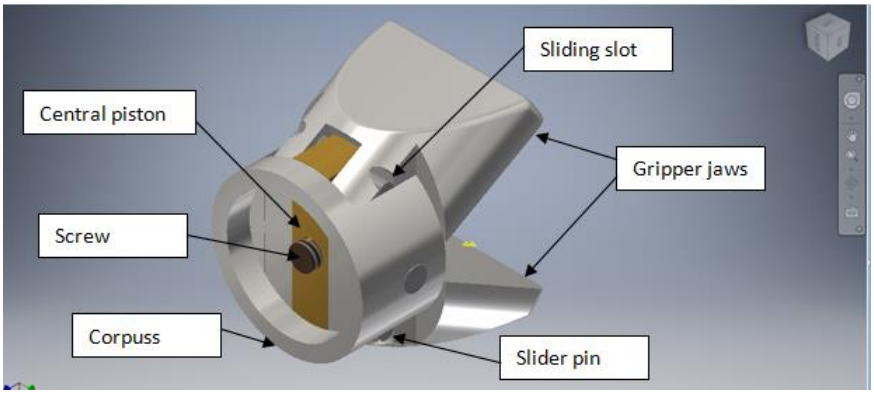

Figure 8. Gripper CAD model

Autodesk Inventor dynamic simulation was performed in order to get required activation force and to get data for critical components strength tests. Model was loaded with constant 6N forces at gripers' jaws tips, what resulted in value of required maximal actuation force of 25N in fully open jaws position at step 99 (**Figure 9**).

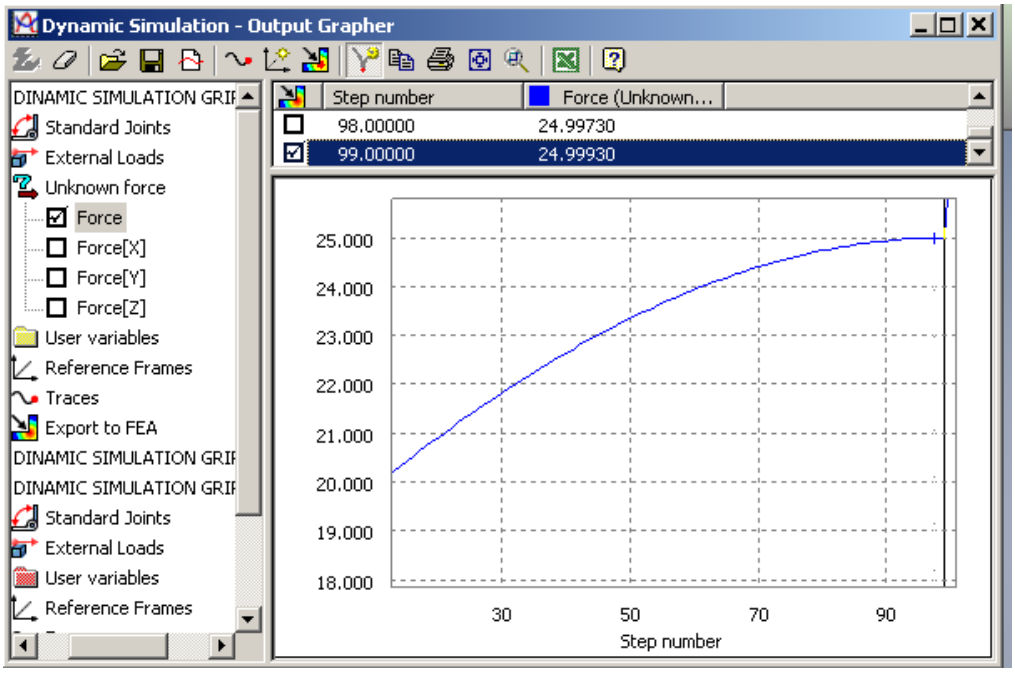

Figure 9. Required actuation force output graph

Maximal actuation force value was later used as an input force in order to perform critical components strength test by exporting data from dynamic simulation into structural analysis environment. Tests revealed satisfactory strength of components, with minimal safety factor value among all components of 2.1 (**Figure 10**), and therefore components should be able to withstand required maximal loads.

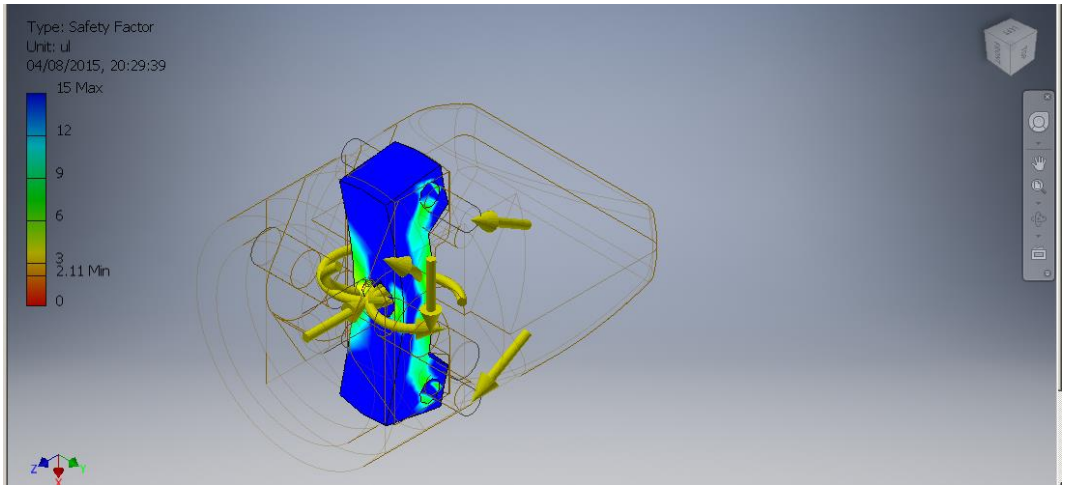

Figure 9. Gripper critical component strength analysis results

3.2 Actuator design

3.2.1 Analysis stage

3.2.1.1 Timing parameters

In order to create appropriate actuation device, suturing task timing must be analysed. The main parameters, which are of interest, are exerted forces, times and position instrument jaws. Summary of these parameters can be found literature [26] and is summarised in**Table6**.

According to suturing task analysis, needle driver most of the time is in closed position, while applying full gripping force, therefore, it can be expected, that self – locking actuator would result in significant power savings. Most appropriate self-locking mechanism for this actuator design must be low pitch screw and nut mechanism, as it can easily be incorporated in grippers design, is simple to design and manufacture, reliable, and low cost. Therefore, actuator should be able to produce rotational output.

Operation	Needle driver operating mode duration, s			Tissue grasper operating mode duration, s		
Tissue grasper positioning	Closed (Maximal force)	Open (Minimal force)	Transitional *	Closed (Maximal force)	Open (Minimal force)	Transitional *
Bite the tissue	0.5					1
Needle positioning	51			51		
Pierce the tissue	20			20		
Release the bite			1	0.5		
Position the grasper		13		13		
R e bite the needle			1	0.5		
Pull needle with thread		17		17		
Release the tissue	0.5					1
Total duration	92	30	2	102	20	2
Average percentage of time in closed position, s					78.9	
Average percentage in time open position, s					20.3	
Average percentage in time Transitional position, s					0.8	
Average full cycle frequency, Hz					0.008	

Table 6. Gripper operation timing parameters during inracorporeal suturing

3.2.1.2 Environmental conditions and safety

In addition to analysis findings, described chapter 3.1.1.1**,** actuator assembly will contain active elements, which can be more sensitive than gripper assembly, and should not be exposed to environment during surgery and sterilisation. Therefore, actuator active elements should be sealed from environment, and should not be damaged during at least low temperature sterilisation.

Pressurised gas, which is used to create pneumoperitoneum, can create pressure difference between the operating room and the body cavity. As a result, the device must be able to withstand pressure changes when it is inserted and removed from the body cavity.

Device outer casing should not reach unsafe temperatures.

3.2.1.3 Design specification

Diameter should not exceed 12mmm

Outer casing should have structures for mounting to robotic arm

Length - as short as possible

Outer casing material - Stainless steel 316

Should be able to provide means of feedback about exerted gripping force

Active elements must be sealed from outside environment

Activation energy – electric current

Maximum output force - 25N

Time, required to close/open the jaws -1s

Minimal continuous operating frequency 0.01 Hz

3.2.2 Synthesis stage

3.2.2.1 Design concept development

Hybrid actuator will consist of rotational motor and SMA element, which should be connected in parallel, in order to increase actuator efficiency and minimize possible overheating issues due to low efficiency of SMA element. In addition, overall mass of the SMA element should be as low as possible, what leads into conclusion, that it should be used only for small portion of total actuator's displacement.

Based on these findings, concept of hybrid actuator was developed through multistage process, summarised in **Table10.**

Schematic of design concept	Achieved targets	Possible design issues
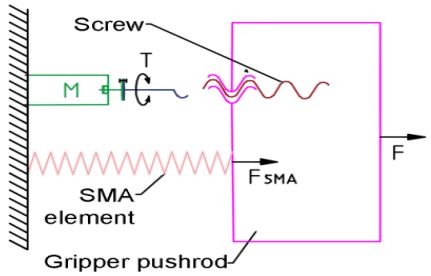	Electric motor and SMA element are connected in parallel	Large mass of SMA element. Overheating issues are possible.
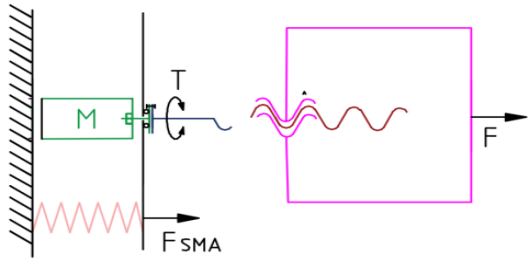	Mass of SMA element is minimal	SMA element should remain active as long as maximal force output is needed. Overheating issues are possible.
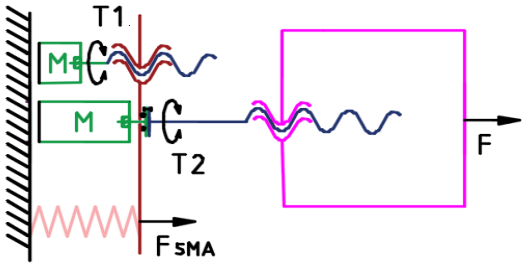	SMA element is only active for short period of time, risk of possible overheating is minimised	Second source of rotational output with correct timing is needed, design can be too complex/bulky
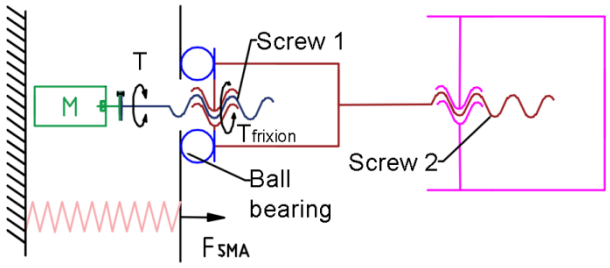	Need for second source of rotational output is eliminated	

Table 7. Process of hybrid actuator design concept development

Design concept was adapted to required cylindrical shape of the actuator. In addition, single SMA element was replaced by array of 6 SMA springs that are placed close to device outer casing in order to minimise heat accumulation and therefore maximise possible operating frequency. SMA spring elements were used in order to minimise device length. Schematic look of developed actuator design is shown in **Figure 10**.

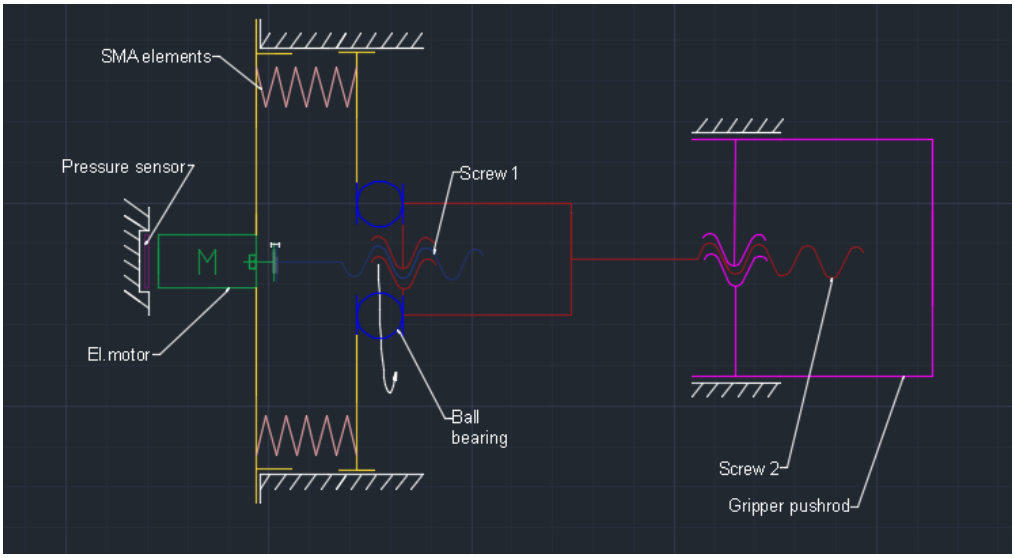

Figure 10. Schematic look of developed actuator design

3.2.2.2 Actuator operation

Forward movement, closing the gripper jaws.

Initial conditions F0 **(Figure 11)**

SMA elements are fully compressed, and exerts force $F_{SMACOLD}$, which results in equal and opposite reaction force $R_{SMACOLD}$, and in turn results in frictional moments T_{S1-2} and $T_{BB.}$, due to friction in ball bearing, and screw joint between Screw 1 and Screw 2 contact surfaces.

Actuator load $F \approx 0$, as gripper is in fully open position, and there is no load on gripper jaws

Force, exerted on pressure sensor, $R \approx 0$

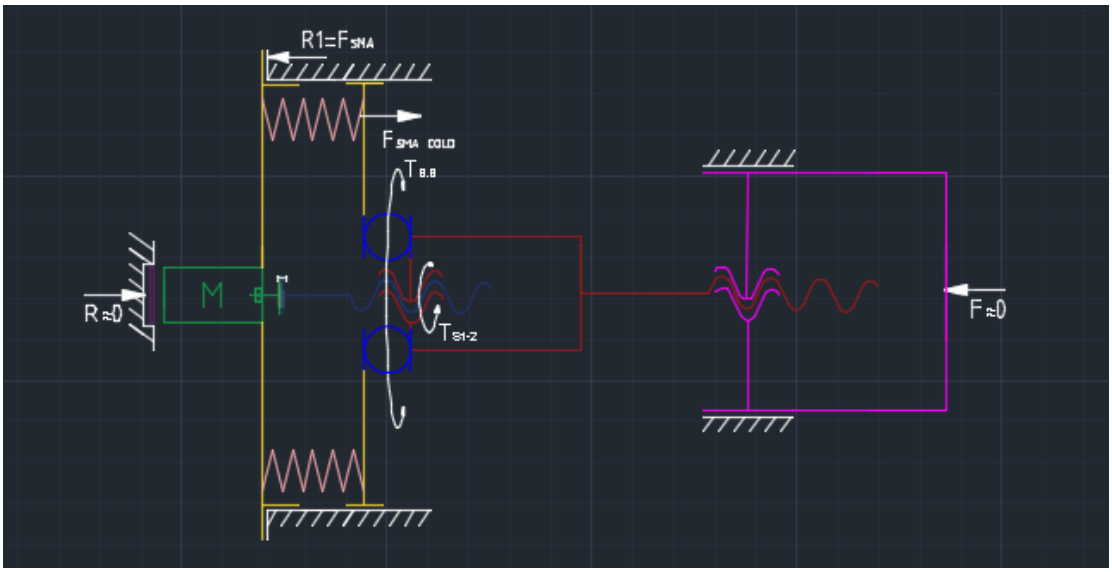

Figure 11. Actuator operation, initial conditions

Event F1 **(Figure 12)**

Electric motor is activated by reverse polarity current, and starts to exert its specific counter clockwise stall torque T_0 on screw 1.

$T_0 = -T_{STAL}$

Because frictional moment absolute value T_{S1-2} is greater than sum of frictional moment T_{BB}, inertial moment T_{IN}, which occurs due to device parts acceleration, and moment, required for **Screw 2** rotation, T_{RISE}, no movement occurs at **Screw1 –Screw 2** joint. Therefore booth of them starts to rotate with this same counter-clockwise angular velocity. Gripper pushrod moves forward, jaws start to close:

$$|T_{S1-2}| > |T_{BB} + T_{IN} + T_{RISE}|$$

$$\omega_1 = \omega_0 \neq 0$$

$$V \neq 0$$

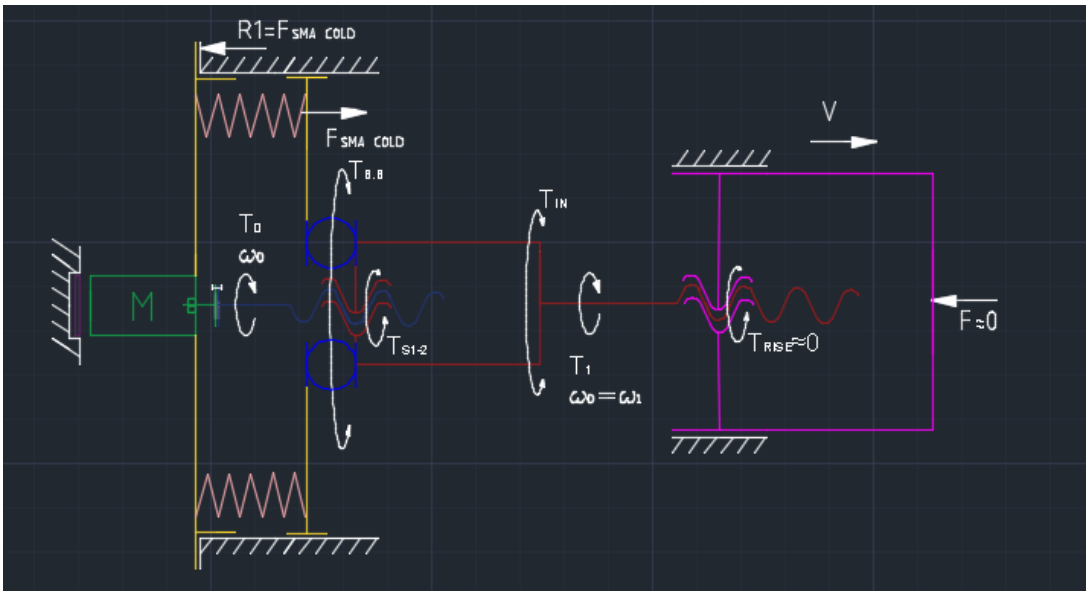

Figure 12. Actuator operation, Event F1

Event F2 **(Figure 13)**

Gripper jaws starts to grab the object or fully close, what in turn leads into steep rise in force, required to continue closing the jaws, and required torque T_{RISE}, which eventually becomes larger than maximal electric motor torque, and **Screw 2** stops rotating.

Rising force F results in equal and opposite reaction force R, exerted on electric motor – pressure sensor contact surface.

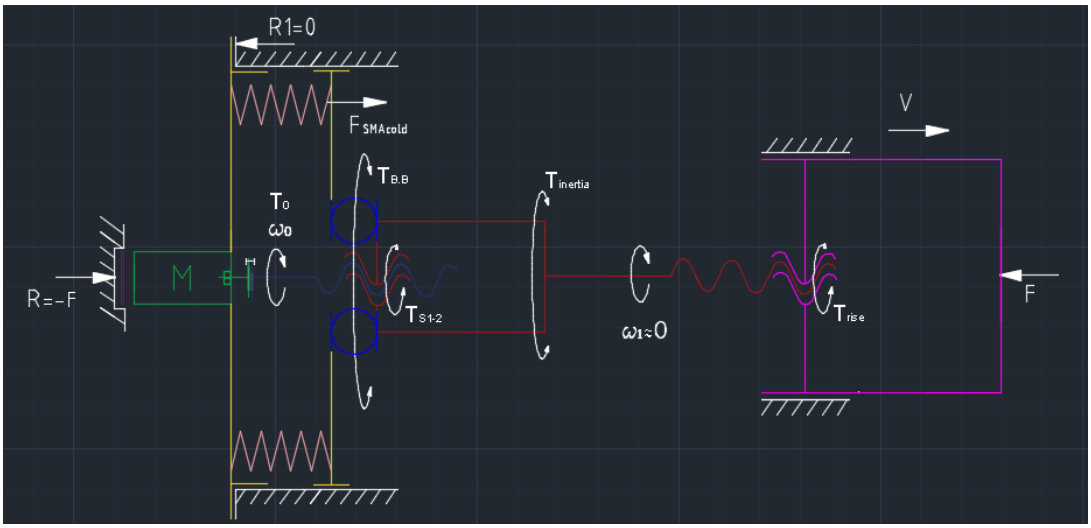

Figure 13. Actuator operation, Event F2

Event F3 **(Figure 14)**

Pressure rise in electric motor – pressure sensor contact surface in turn leads into changes in pressure sensor resistivity, specific value of which triggers SMA elements heating current activation.

SMA elements heating results in force $F_{SMA\ HOT}$, which further increases actuator force output, and decreases force, acting in screw 1 –screw 2 screw joint.

Because T_{RISE} is now much larger thanT_{S1-2}, motor torque causes **Screw 1** to rotate, while **Screw 2** is stationary, what in turn, together with $F_{SMA\ HOT}$ hot gives maximal actuator force F_{MAX}

$$F_{SMA\ HOT} + F_{MOTOR} = F_{MAX}$$

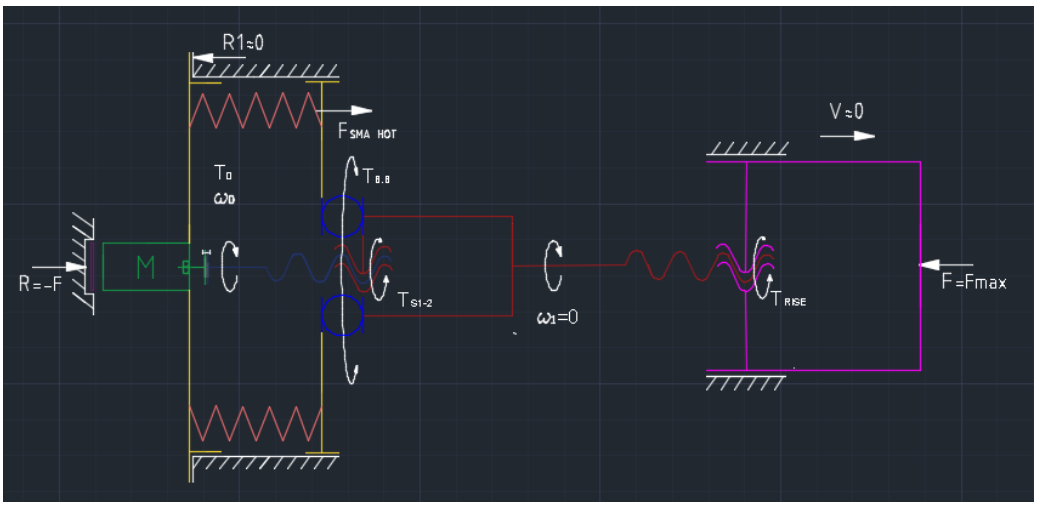

Figure 14. Actuator operation, Event F3

Event F4 **(Figure 15)**

F_{MAX} results in equal and opposite reaction force, R_{MAX}, at electric motor – pressure sensor contact surface what in turn leads into further changes in pressure sensor resistivity, specific value of which in turn triggers power switch off for all, electric motor and SMA elements.

Gripper is now locked in closed position, and exerting close to maximal force. SMA elements start to cool.

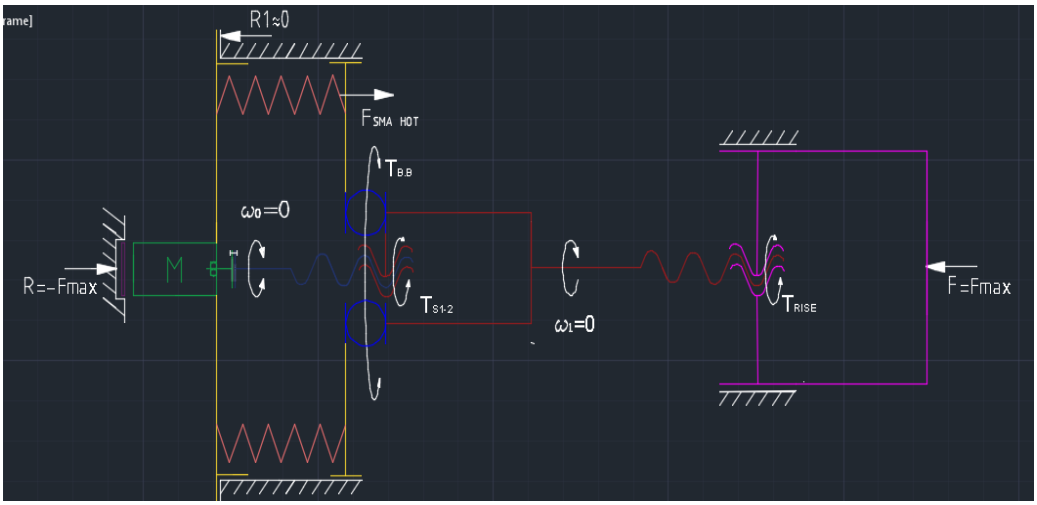

Figure 15. Actuator operation, Event F4

Reverse

Initial conditions R0 **(Figure 16)**

Actuator load $F \approx F_{MAX}$, as gripper is in closed position, and exerts maximal force.

SMA elements are fully extended, and exerts force F_{SMA}. Force, exerted on **Screw 1-Screw2** joint, $(F_{MAX} - F_{SMA\ COLD})$ results frictional moments $T_{S1-2\ LOWER}$ and $T_{BB.}$,due to friction in ball bearing and screw joint between **Screw 1** and **Screw 2** contact surfaces.

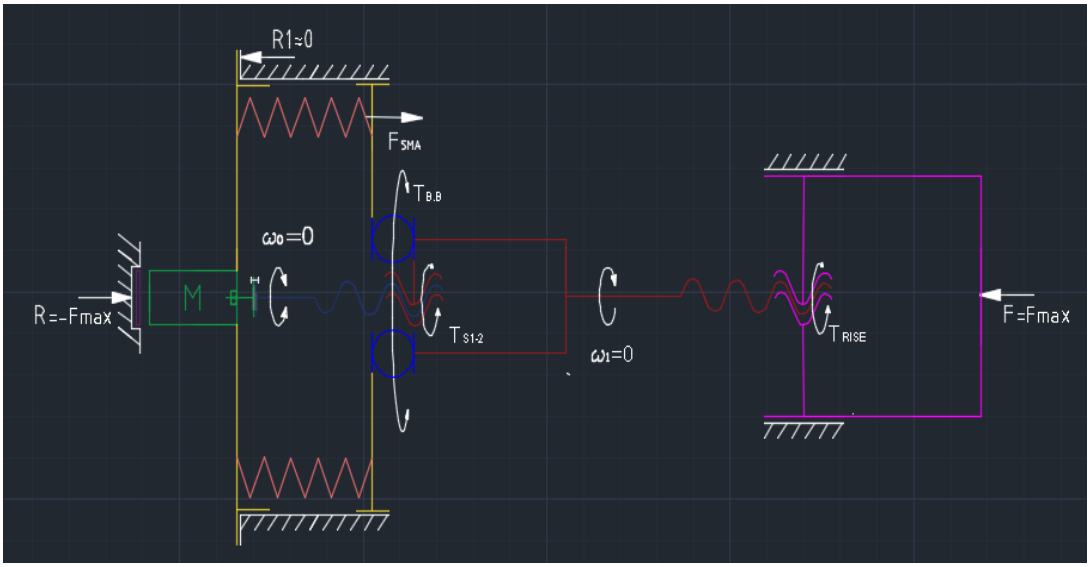

Figure 16. Actuator operation, Event R0

Event R1 **(Figure 17)**

Electric motor is activated by correct polarity current, and starts to exert its specific clockwise stall torque on screw 1.

$T_0 = T_{STAL}$

Because frictional moment required to compress SMA elements, $T_{S1-2\ LOWER}$ is lower than T_{STAL}, **Screw 1** starts to rotate in clockwise direction, what results in

rapid decline in actuator force F, what in turn leads in decline in required torque T_{RISE}, and frictional moment T_{BB}.

$T_{S1-2\ LOWER} < T_{STAL}$

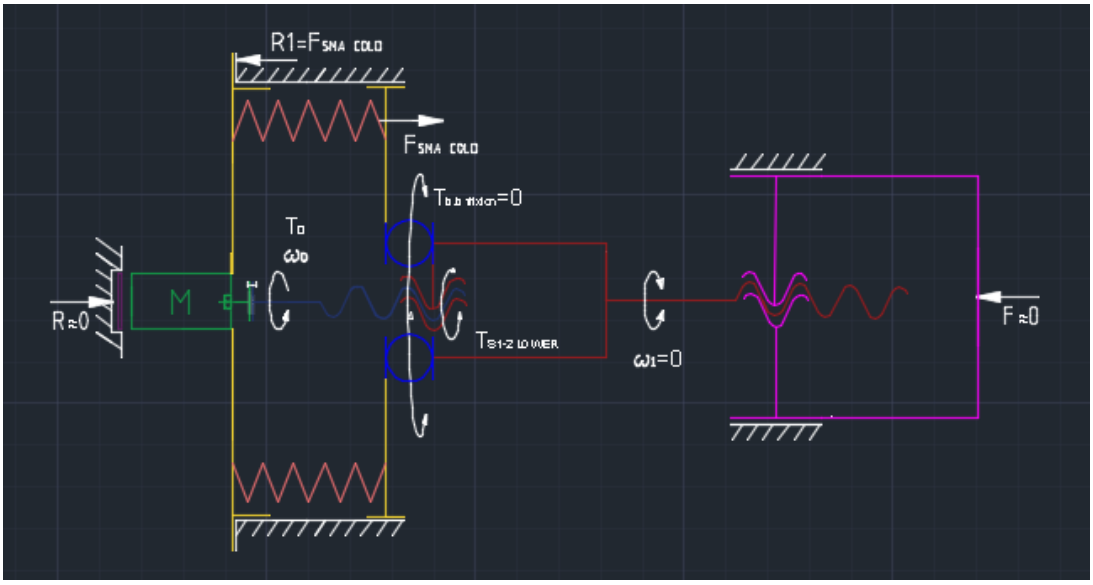

Figure 17. Actuator operation, Event R1

Event R2 **(Figure 18)**

As soon as T_{LOWER} becomes lower than T 1-2, screw 2 starts to rotate with this same angular velocity as **Screw1** , and gripper jaws open.

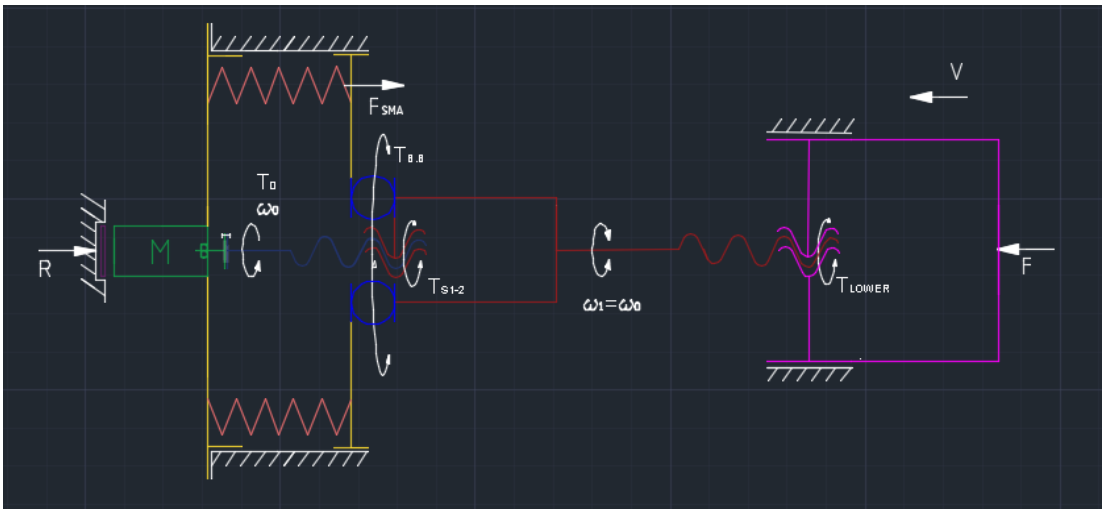

Figure 18. Actuator operation, Event R2

Event R3 **(Figure 19)**

Gripper jaws reaches fully open position, where screw 2 rotation is mechanically stopped.

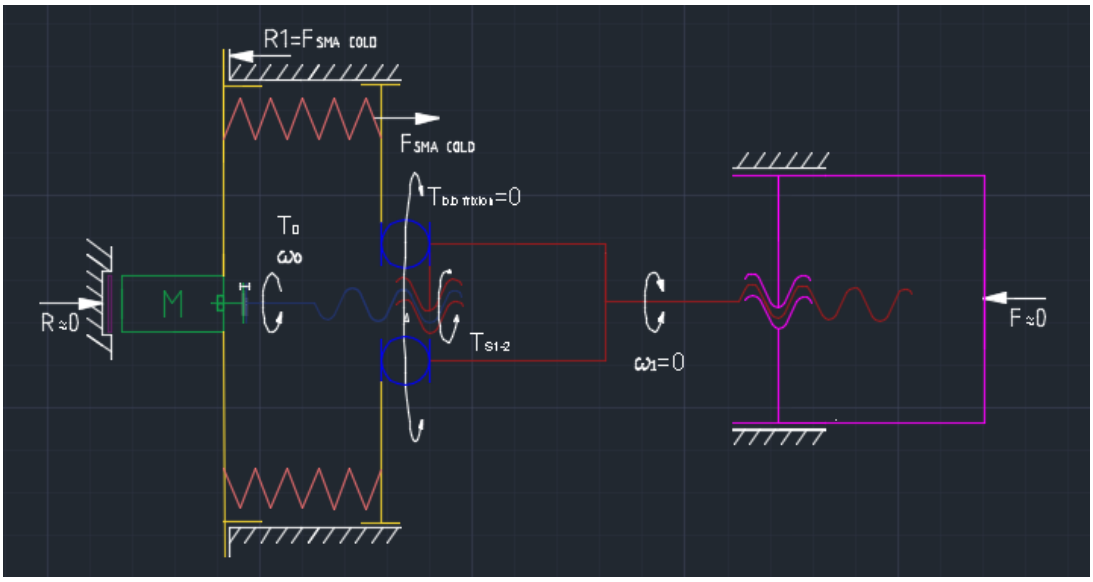

Figure 19. Actuator operation, Event R3

Event R4 **(Figure 20)**

Because maximal electric motor torque T0 is larger than the torque, required to compress now cooled SMA elements due to screw1 rotation, $T_{SMA\ COMPRESS}$, rotation continues until the SMA elements are fully compressed and full actuation cycle is completed and electric motor driving current is switched off. Because pressure sensor cannot provide information about state of the actuator, current switch of should be triggered after certain period of time, which could be determined experimentally.

$T_{SMA\ COMPRESS} < T_{STALL}$

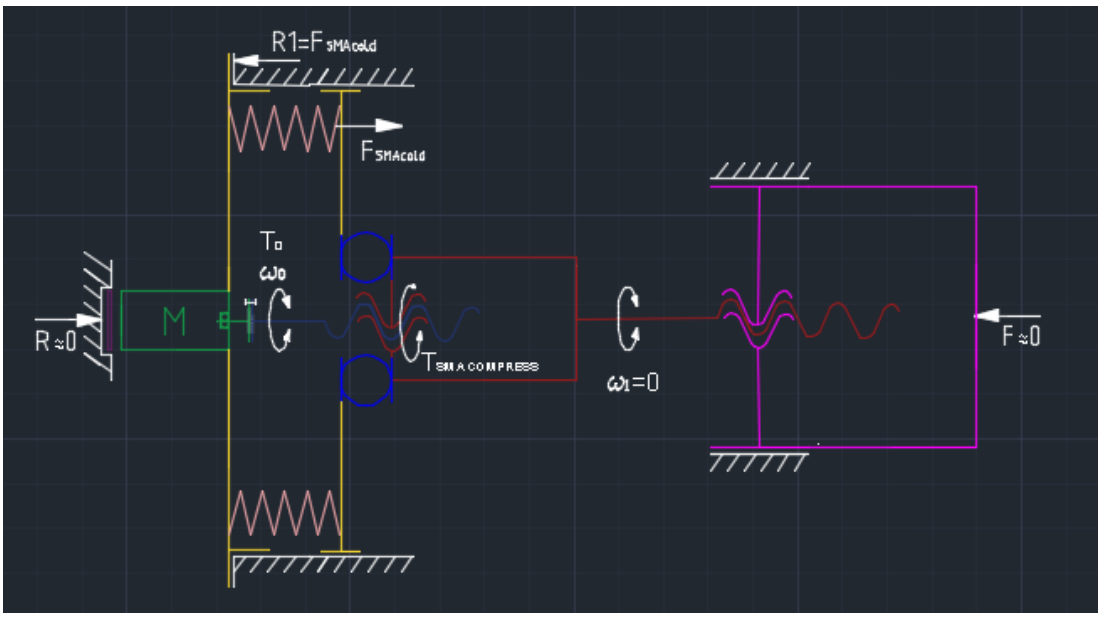

Figure 20. Actuator operation, Event R5

Summary of critical conditions, that should be satisfied for proper device operation:

$$|T_{S1-2}| > |T_{BB} + T_{IN} + T_{RISE}|$$

$$F_{SMA\ HOT} + F_{MOTOR} = F_{MAX}$$

$$F_{MAX} = 25N$$

$$T_{S1-2\ LOWER} < T_{STAL}$$

$$T_{SMA\ COMPRESS} < T_{STALL}$$

Corresponding equations that describe values of critical conditions:

Frictional moment value T_{S1-2} (Event F1) [27]

$$T_{S1-2} = \frac{F_{SMA\ COOL} d_m}{2} \left(\frac{l - \pi f d_m sec\alpha}{\pi d_m + l f l sec\alpha} \right) \quad (1)$$

$$d_m - \ medial\ diameter\ of\ screw, mm$$

$$f - coeficient\ of\ frixion$$

$$\alpha - thread\ angle$$

$l - lead, mm$

Force, exerted by cool and compressed SMA elements [19]:

$$F_{SMA\ RESET} = n\delta_L K_L \quad (2)$$

Low temperature spring deflexion:

$$\delta_L = \delta_H + stroke \quad (3)$$

High temperature spring deflexion:

$$\delta_H = \frac{F_{SMA\ HOT}}{K_H} \quad (4)$$

High temperature spring index:

$$K_H = \frac{G_H d^4}{8nD^3} \quad (5)$$

d −Diameter of sma spring wire

D − medial diameter of SMA spring

Number of SMA springs:

$n = 6$

Low temperature spring index:

$$K_L = \frac{G_L d^4}{8nD^3} \quad (6)$$

Maximal force, produced by SMA elements:

$$F_{SMA\ HOT} = \frac{nd^2\pi\tau_C}{8WC} \quad (7)$$

Maximum allowed shear stress of SMA elements [28]:

$\tau_C = 160MPa$

Spring ratio:

$$C = \frac{D}{d} \quad (8)$$

Wahl correction coefficient:

Inertial moment due to Screw 2 mass acceleration (Event F1):

$T_{IN} \approx 0$

Torque, required to close the gripper jaws with no external load:

$T_{RISE} \approx 0$

Maximal force, which can be produced due to motor torque, exerted on screw 1 (Event F3)

$$F_{MOTOR} = \frac{T_{MAX}}{d_m}\left(\frac{\pi d_m - f l sec\alpha}{l + \pi f d_m sec\alpha}\right);$$

Torque, required to initiate gripper release (Event R1):

$$T_{S1-2\ LOWER} = T_L = \frac{F_{MAX} - F_{SMA\ COOL} d_m}{2}\left(\frac{l + \pi f d_m sec\alpha}{\pi d_m - f l sec\alpha}\right)$$

Torque, required to compress cooled SMA elements:

$$T_{SMA\ COMPESS} = \frac{F_{SMA\ COOL} d_m}{2}\left(\frac{l - \pi f d_m sec\alpha}{\pi d_m + l f l sec\alpha}\right);$$

Based on critical conditions and corresponding equations, electric motor, dimensional and material properties of SMA elements, ball bearing, Screw 1, and Screw 2 were chosen and calculated (**Table 8**).

$$W = \frac{4C-1}{4C-4} + \frac{0.615}{C} \quad (9)$$

Frictional moment value T_{BB} (Event F1) [27]:

$$T_{BB} = f_{BB} * R_m * F_{SMA\ COLD} \quad (10)$$

Friction coefficient in ball bearings:

$f_{BB} = 0.001$

R_m −Medial diameter of ball bearing

Design element	Properties of elements	Value
Screw 1	$Diameter\ of\ screw\ 1\ (metric)$	1mm
	$l - lead, mm$	0.2mm
	Material	Stainless steel
Screw 2	$Diameter\ of\ screw\ 2\ (metric)$	1.6mm
	$l - lead, mm$	0.35mm
	Material	Bronze
SMA elements	d −Diameter of sma spring wire	0.5mm
	D − medial diameter of SMA spring	1.7mm
	Number of turns	1.5
	Material	NiTinol, Dynalloy
	Number of springs	6
	SMA elements	d −Diameter of sma spring wire
Ball bearing	Diameter	3mm
Maxon flat series motor 301999 [29]	Maximum torque output	0.4nNm
FSR 149 pressure sensor [30]	Load range	10-100N

Table 8. Properties of actuator elements

3.2.2.3 Device control and feedback

Control system should provide SMA elements and DC motor currents with correct timing in order to ensure proper operation of the device.

Integrated microcontroller can be used for currents control, however, driving signals from commercially available microcontrollers in general are only capable to provide low power signals, and therefore should be not connected directly to high power elements. In addition, SMA elements and electric motor will require different voltages and currents. Therefore, driving signals will be connected to transistor H bridges, which will provide required currents and voltages for actuator active elements. $Arduino\ \mathrm{Uno}^{R}$ integrated microcontroller, connected to H bridges will be used in this work.

Control of brushless DC motors in general is more complicated than brushed DC motors. The motor, used in this project has three electromagnetic pairs, which should receive current of correct polarity and timing in order to produce rotational output. In this project this will be achieved by using$Precision\ Microdrives^{TM}$ brushless motor driving module, based on Texas Instruments DRV11873 microchip, which do not requires input from motor hall sensor. This device will be responsible for generation of appropriate currents, and will operate in constant duty. On/Off regimes will be achieved using transistor H bridge, which will activate or deactivate electric power supply to DC motor control board. Forward/Reverse regimes will be achieved using dedicated jumper pins on motor driving module.

Pressure sensor will be connected to Wheatstone bridge in order to achieve more accurate timing. In addition, bridge output voltage will provide feedback on exerted gripping force.

Therefore control system will consist of integrating microcontroller, two transistor H bridges, brushless DC motor control circuit, Wheatstone bridge and pressure sensor. Block diagram of device control system is shown in **Figure 21**.

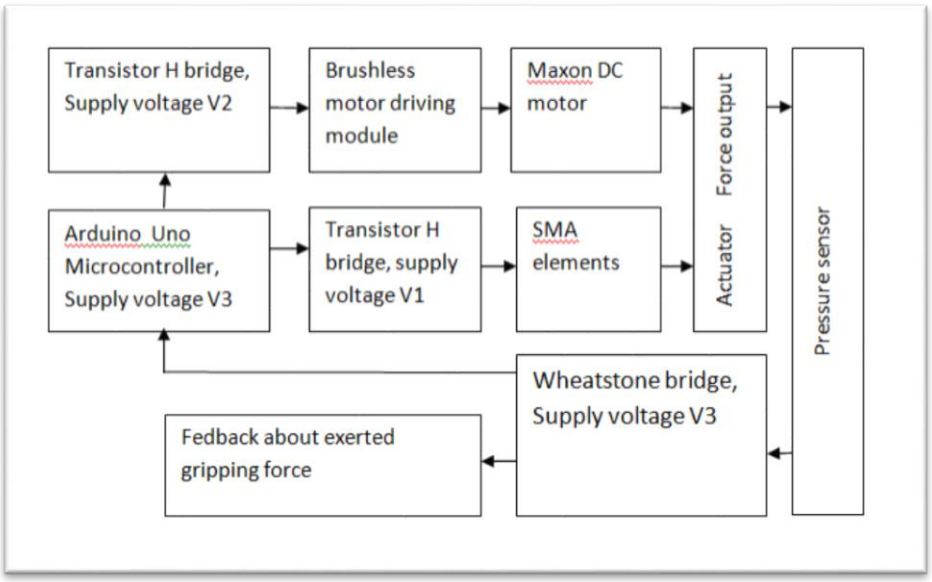

Figure 21. Block diagram of device control system

3.2.3 Evaluation stage

In order to test design suitability, actuator CAD model was created using Autodesk Inventor software. CAD model sectional view can be seen in **Figure 22**.

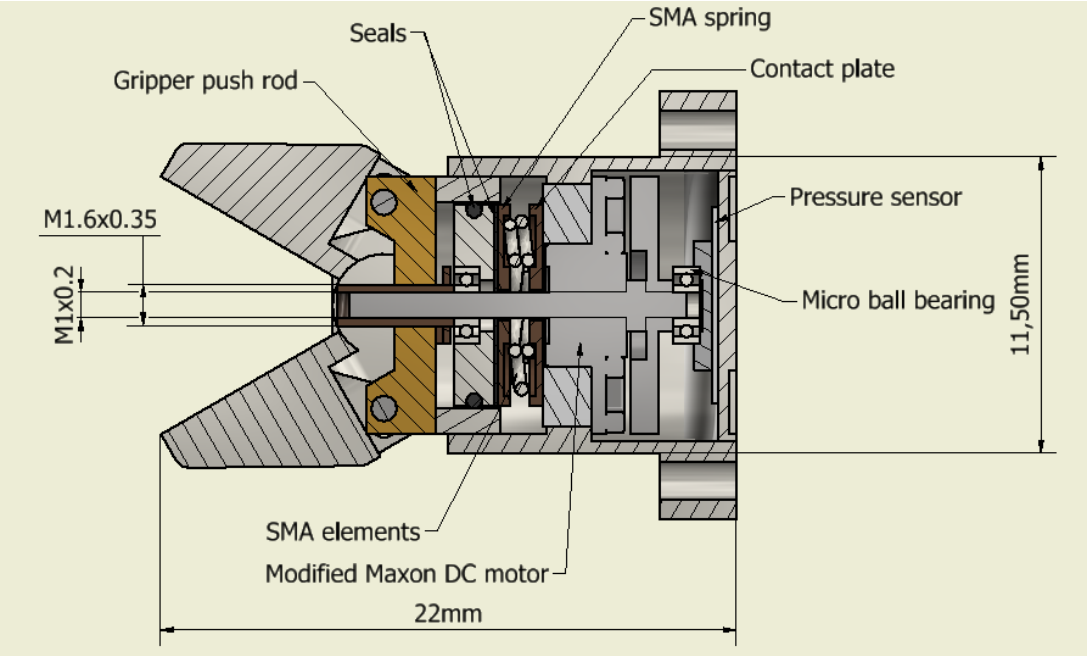

Figure 22. Device design sectional view

Maximal actuation force value (25N) was used as an input force in order to perform critical components strength using Autodesk Inventor structural analysis environment. Tests revealed satisfactory strength of components, with minimal safety factor among all components of 1.35 (**Figure 23)**, and therefore all components should be able to withstand required maximal load.

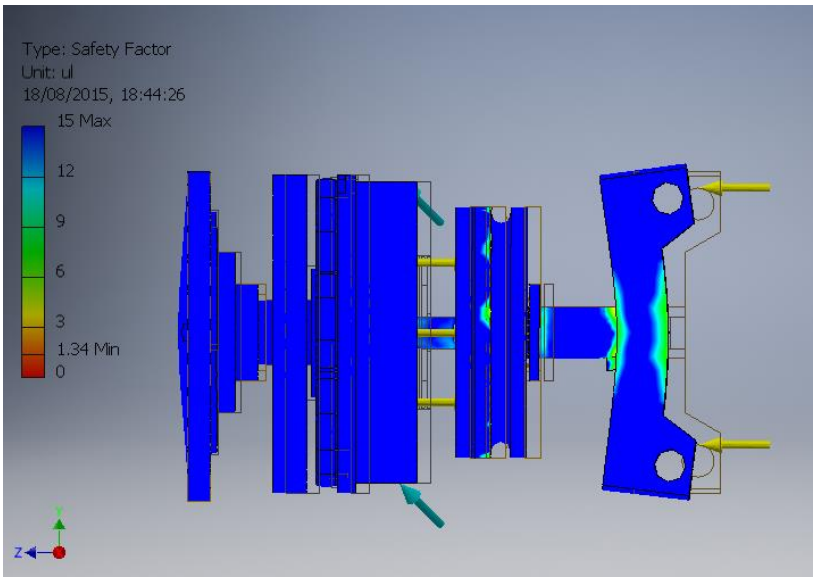

Figure 23. Critical component strength analysis results

3.2.3.1 Thermal behaviour of the actuator

Actuator performance will depend on heating and cooling processes, and its elements will reach high temperatures, therefore analysis of actuator thermal behaviour is necessary in order to proof it will operate properly, and will be safe to use. Analysis of thermal behaviour was performed using Autodesk CDF software.

Firstly, steady state analysis was performed in order to get device maximum operating frequency, while its outer casing elements do not reach unsafe temperatures and its elements do not reach temperatures above NiTi full austenitic temperatures.

Analysis inputs:

Analysis type – Steady state

Outside volume – 1L of CO2, device is located at the centre of volume, in horizontal position.

Initial temperature of all elements -$37°C$

Constant Outside volume boundaries temperature -$37°C$, as it is considered, that body tissues have large heat capacity in compare with device heating power.

Temperature dependant heat transfer from device outer casing by free convection

Temperature dependant heat transfer from device outer casing by heat radiation

Total heat generation power of electric motor:

$P_1 = 0.05W$

Total heat generation of SMA elements:

$$P_2 = Qf_{max} \quad (11)$$

Where

Amount of energy, required to rise SMA elements temperature from full martensitic to full austenitic state [28]:

$$Q = c_p m(T_2 - T_1) \quad (12)$$

NiTinol Specific heat [29]:

$$c_p = 0.837 J/(gC°)$$

Overall mass of SMA elements, taken from device CAD modelling software:

$$m_{SMA} = 0.047 g$$

SMA full austenitic temperature:

$$T_2 = 90°C$$

SMA full martensitic temperature:

$$T_1 = 50°C$$

$$QP_2 = 0.837 * 0.047 * (90 - 50) = 1.8 J$$

Analysis results are shown in **Figure 24** and **Figure 25**.

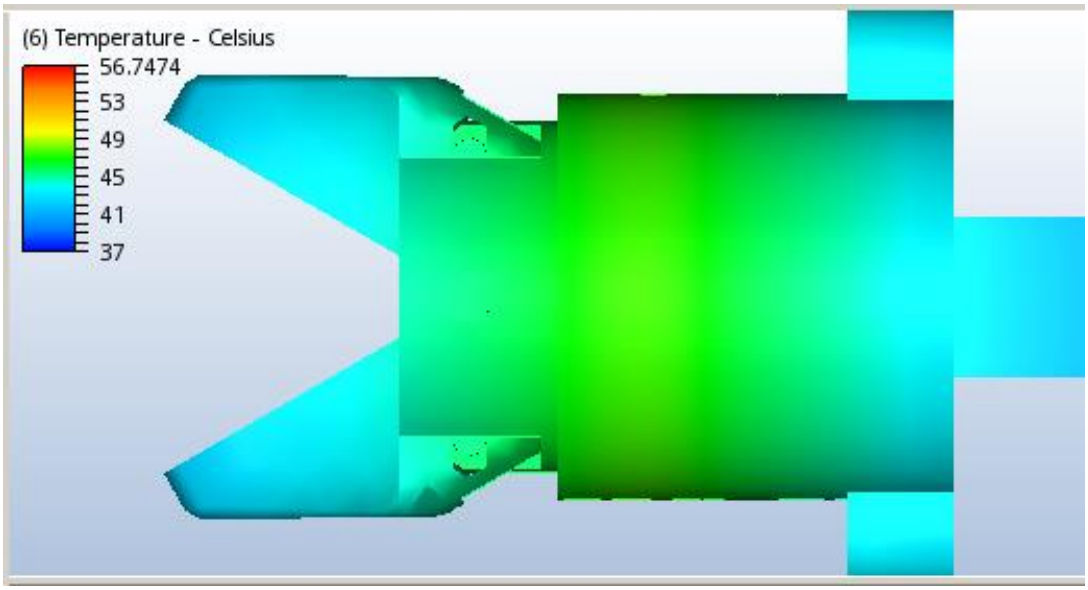

Figure 23. Device outer elements steady state temperature map

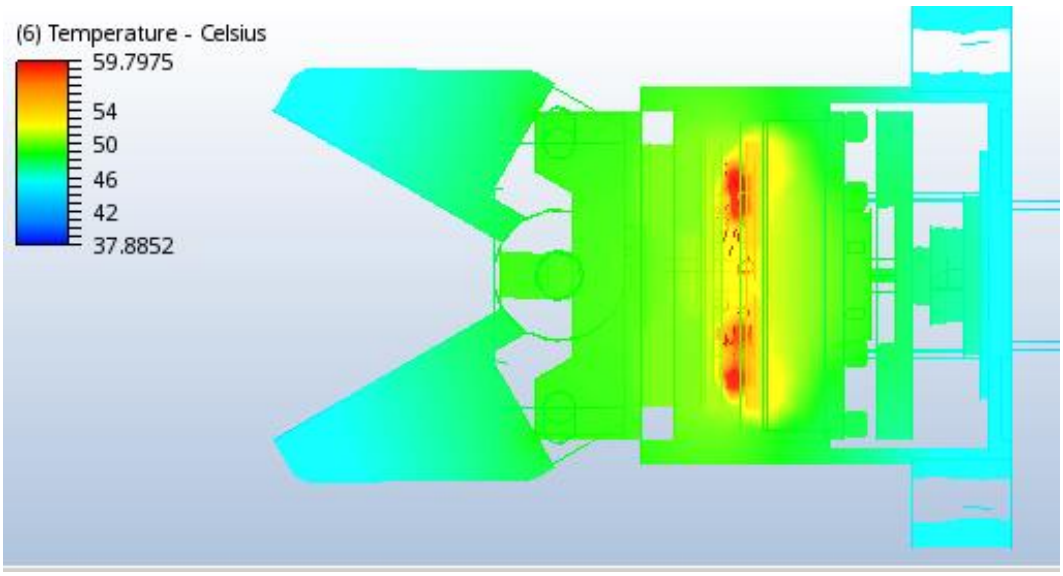

Figure 25. Device inner elements steady state temperature map

Maximal full cycle device operating frequency was found by trial and error method, by changing total heating power of SMA elements until steady state temperatures of device were not higher than relatively safe $52°C$. Which was found to be 0.35W.

Therefore, device maximum continuous operating frequency:

$$f_{max} = \frac{Q}{0.35} = 0.19Hz \quad (13)$$

Which is much higher, than that found in suturing task analysis in **Table1** (0.008Hz), and device should be suitable for performing intracoporeal suturing tasks.

Because the SMA will be activated only once during entire cycle and activation time is expected to be very short in compare with duration of inactive period, cooling effects, which occurs during SMA activation, is expected to be minimal, and were not included in this analysis.

Next, steady state temperatures of device components where used for SMA elements cooling speed analysis in order to proof, that they can cool fast enough to full austenitic temperature when device operates at maximal frequency.

Analisis inputs:

Analysis type - Trasitient

Analysis duration - 5s

Outside volume – 1l of CO2, device is located at the centre of volume, in horizontal position

Constant Outside volume boundaries temperature - 37C, as it is considered, that body tissues have large heat capacity in compare with device heating power.

Temperature dependant heat transfer from device outer casing by free convection

Temperature dependant heat transfer from device outer casing by heat radiation

Total heat generation power of electric motor:

$P_1 = 0.05W$

Total heat generation of SMA elements:

$P_2 = 0$

Analysis results are shown in **Figure 26.**

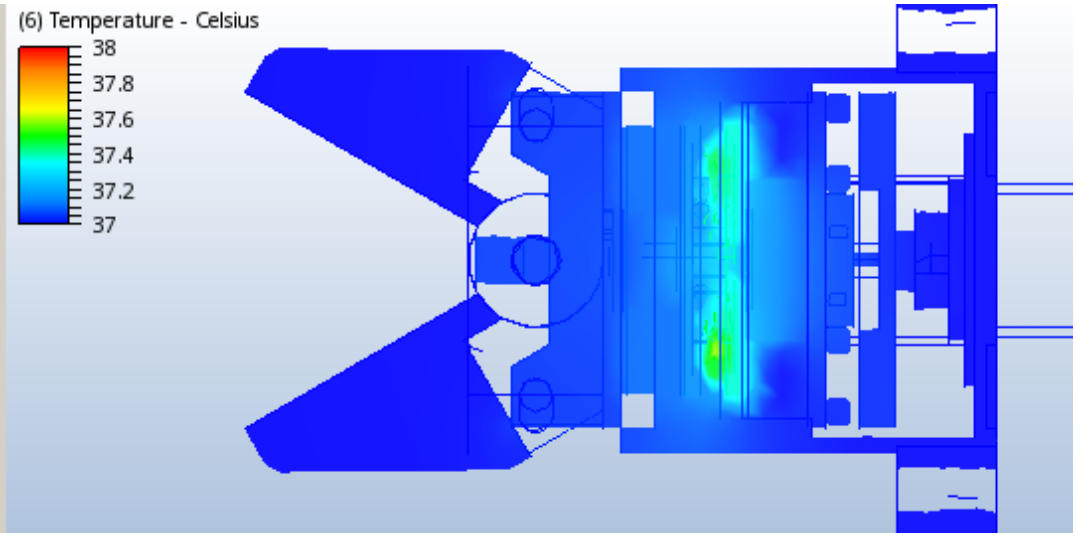

Figure 26. Temperatures of device internal elements after 5s from inactivation

4. Prototype manufacturing and assembly

Non-standard device parts were manufactured using Proxxon mini milling/drilling machine, and conventional metal machining techniques.

Several design simplifications were applied in order to reduce complexity machining time, as they were unlikely to affect device performance during planed testing:

- Aluminium instead of stainless steel was used for actuator outer casing.
- Mounting structures, which should be used for device attachment to robotic arm, were not machined.
- Outside casing cable canal was not machined.
- Complex shape of gripper jaws was simplified in order to reduce machining time.
- Gripper jaws were modified in order to provide place for force sensor placement during testing.

- All device sealing parts were not used.

Manufactured gripper assembly can be seen in **Figure 27**.

Figure 27. Gripper assembly

Maxon flat series motor 301999 was modified by replacing original output shaft with custom made one, in order to make possible axial loading on motor assembly. In addition, custom motor shaft has 1mm metric tread, which was used in order to further reduce device length and complexity. Motor was tested after modification, in order to proof it was not damaged during the modification process. Modified Maxon motor can be seen in **Figure 28.**

Figure 28. Modified Maxon DC motor

Insulation plate vas secured on Maxon motor with the small amount of Locktite 638 glue, together with bottom contact plate. Bottom contact plate was then covered with small amount of thermal grease and 6 SMA springs were then placed in dedicated contact plate's pits. Top contact plate mounted and secured with the help of top micro ball bearing and Screw 2. Manufactured hybrid actuator assembly can be seen in **Figure 29**.

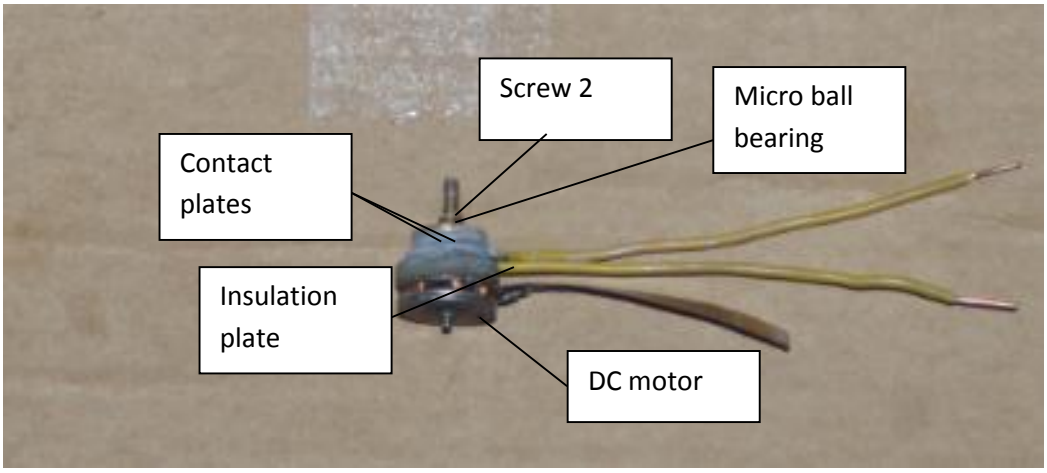

Figure 29. Hybrid actuator assembly

Actuator assembly was then placed in device outside casing. Gripper assembly was fully closed, and mounted on actuator assembly output screw 2, then gradually screwed in outer casing. When the gripper reached fully closed position. Maxon motor was manually rotated clockwise, to open the jaws. Then, gripper assembly was screwed in its final position, and gripper jaws manually open by again manually rotating Maxon motor. Finally, bottom ball bearing, pressure plate and FSR 149 pressure sensor were placed and secured with the help of bottom plate. Fully assembled device can be seen in **Figure 30.**

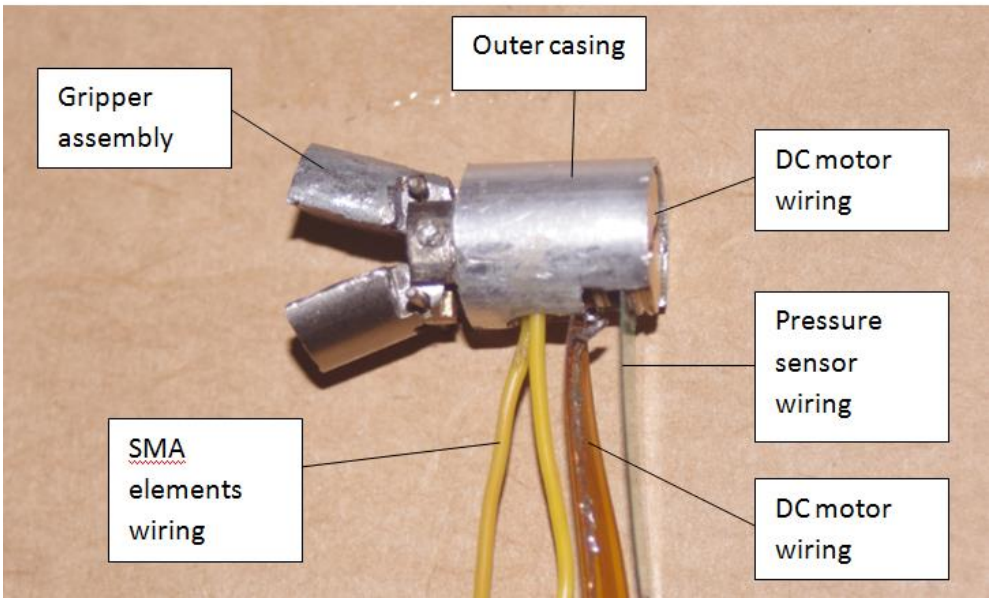

Figure 30. Fully assembled prototype

5. Prototype testing

5.1 Testing setup

Gripping force was one of the main parameters that are of interest during prototype testing, therefore force sensor was also designed and manufactured in order to evaluate device performance. FSR 149 pressure sensor, similar to that, used in actuator, was used an active element in sensor design. 0.5mm thickness and 5mm in diameter plate, made from Derlin plastic was attached to sensor in order to apply pressure, exerted by gripper jaws on active area of pressure sensor. Plates were attached to sensor with ultra-thin double side sticky tape. Sensor assembly was than attached to gripper jaw with small amount of Locktite 638 glue, and calibrated by applying known weight on freely movable gripper jaws, using Wheatstone bridge and Hantek PC o for output voltage values measuring. Pressure sensor, mounted on gripper assembly can be seen in **Figure 30.**

Figure 30. Gripper assembly with mounted force sensor

Prototype was mounted in vertical position, and wired to required electric and electronic hardware. Force sensor was connected to Wheatstone bridge, which was in turn connected to Hantek PC oscilloscope. In addition, oscilloscope was also connected to prototype pressure sensor Wheatstone bridge, in order to proof it is capable to provide feedback on produced gripping force. Testing setup can be seen in **Figure 31.**

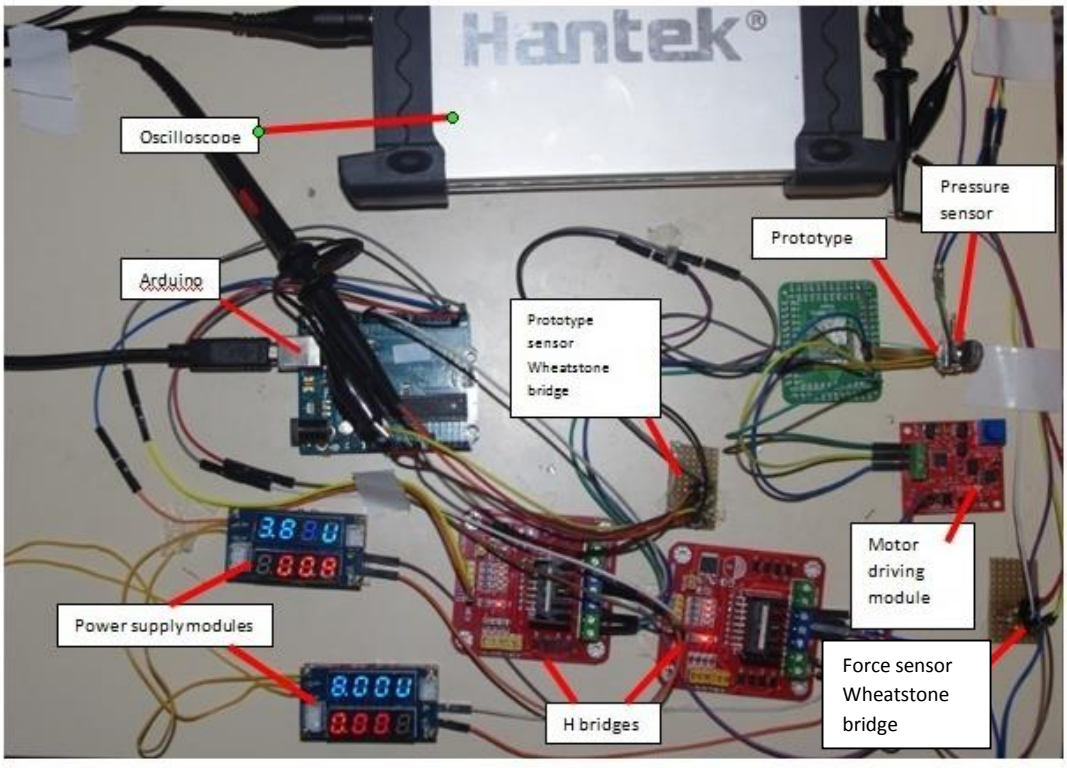

Figure 31. Prototype testing setup

5.2 Testing outcome

Manufactured prototype during testing did not operate properly, as DC motor was not able to provide rotational output. Electrical tests showed, that motor driving currents are supplied to motor. Further motor inspection revealed, that motor wiring was mechanically damaged during assembly process, and one of three motor electromagnetic pairs has no contact with motor wiring ribbon. Repair was attempted, however with no success, and therefore further device performance testing was impossible.

6. Conclusions

This thesis novel compact surgical needle driver and its actuator for SILS robotic surgical system was modelled, simulated, manufactured. The device is 24mm in length, and 12m in diameter (without mounting structures). Hybrid DC motor and Shape Memory Alloy actuator, used in device should be able to produce 25N of force, which would let to get required 6N gripping force. According to performance simulation results, the device could operate at continuous 0.19Hz full cycle frequency without overheating in conditions, compatible with these, found during Minimally Invasive Surgery. Pressure sensor, incorporated in the device design, potentially could provide information about produced gripping force, and therefore reduce risk of unintentional tissue damage during suturing.

Device is relatively complex to manufacture, as many parts used in its design, are extremely small and should have high accuracy parameters.

Device physical prototype performance was not tested in this work, due to unintentional mechanical damage to one of the main parts of prototype, a DC motor. Damage occurred during prototype assembly procedure and in careful

handling conditions, what could suggest, that Maxon flat series motor 301999, used in this prototype, could be too brittle for such applications.

6.1 Future work and improvements

Future work should involve device design modification, using DC motor, which would have more robust construction. This would increase durability and reduce risk of inappropriate operation of the device. In addition, use of brushed DC motor would reduce amount of required electronic hardware and make device control less complex.

Device, based on engineering ideas, shown in this work, should be tested in order to proof they are working in real world conditions.

In this work only the end effector of surgical needle driver was designed and manufactured. Most applications of such device in surgical robots potentially would require to use this device together with spherical or rotational joint, for required precise positioning, therefore, future work could also include design of such joint.

Although in this work as an NiTinol SMA spring elements were used, due to their high power density and relatively large strain output, other, more efficient, types of linear actuators could be also used in such designs, and potentially increase device maximal continuous operating frequency.

Pressure sensor, incorporated in sown design, would only be capable to provide actuation force feedback. In order to completely eliminate risk of unintentional tissue damage due to too large gripping force, could be modified by incorporating additional pressure sensors on gripper jaws.

References

[1] K. L. Protopapa, et al., Development and validation of the Surgical Outcome Risk Tool, [Accessed online: June 2015] at: http://www.ncepod.org.uk/pdf/publications/TheSurgicalOutcomeRiskTool.pdf

[2] C. Palanivelu, Art of Laparoscopic Surgery Textbook and Atlas, 2007, p. 3-85.

[3] Venita C. et al,., A comparison of laparoscopic and robotic assisted suturing performance by experts and novices, Surgery, Volume 147, Issue 6, June 2010, Pages 830–839. [Accessed online: June 2015] at: http://www.sciencedirect.com/science/article/pii/S0039606009007156

[4] Irfan H, Ali T, NOTES: The next surgical revolution? International Journal of Surgery, August 2008Volume 6, Issue 4, Pages 273–276,
[Accessed online: June 2015] at:
http://www.journal-surgery.net/article/S1743-9191(07)00151-3/fulltext

[5] Image adapted from [Accessed online: July 2013] from:
http://www.anthonygonzalezmd.com/

[6] Chin-Hsing Kuo, Jian S, Dai Robotics for Minimally Invasive Surgery: A Historical Review from the Perspective of Kinematics, International Symposium on History of Machines and Mechanisms, 2009,
[Accessed online: June 2015] at:
http://download.springer.com/

[7] Intuitive Surgical, Inc., website, [Accessed online: June 2015] at:
http://www.intuitivesurgical.com/

[8] Robotics News Center for AVRA Surgical Robotics Inc., ZEUS Robotic Surgical System, [Accessed online: June 2015]] at:
http://allaboutroboticsurgery.com/zeusrobot.html

[9]Prashanth P. et al., Single-incision laparoscopic surgery - current status and controversies, J Minim Access Surg. 2011 Jan-Mar; 7(1): 6–16.,
[Accessed online: June 2015] at:
http://www.ncbi.nlm.nih.gov/pmc/articles/PMC3002008/

[10] Shane M. et al., Surgical Robotics Systems Applications and visions, 2015, Pages 123-139, Miniature In Vivo Robots for NOTES,
[Accessed online: June 2015] at:
http://download.springer.com

[11] Yao, W. Childs, Peter R., Application of design rationale for a robotic system for single-incision laparoscopic surgery and natural orifice transluminal endoscopic surgery, Journal of Engineering in Medicine July 2013, vol. 227 no. 7 821-830,

[Accessed online: June 2015] at:
http://pih.sagepub.com/content/227/7/821.refs

[12] Figure adapted from "Surgical Laparoscopy" edited by Karl A. Zucker, 2000,

[13] Manickam R., et al., Comparison of Continuous and Interrupted Suturing in Laparoscopic Pyeloplasty, JSLS. 2014 Apr-Jun; 18(2): 294–300,
[Accessed online: June 2015] at:
http://www.ncbi.nlm.nih.gov/pmc/articles/PMC4035643/

[14] Figure adapted from, Pocket guide to suture materials techniques and knots,
[Accessed online: June 2015] at:
http://www.fmdental.pl/uploads/20110107131642.pdf

[15] Prototypic force feedback instrument for minimally invasive robotic surgery Ulrich S, Bernhard K, Gerd H., Institute of Robotics and Mechatronics, 2007,
[Accessed online: June 2015] at:
www.intechopen.com/books/medical_robotics/prototypic_force_feedback_instrument_for_minimally_invasive_robotic_surgery

[16]The basics of sterilisation, 2007, [Accessed online: June 2015] at:
http://www.casemed.com/caseacademy/downloads/CASDF003.pdf

[17] Chowdhary K. et al., Design and characterization of a novel hybrid actuator using shape memory alloy and DC motor for minimally invasive surgery applications, Mechatronics and Automation, 2005 IEEE International Conference (Volume:1),
[Accessed online: June 2015] at:
http://ieeexplore.ieee.org/xpls/icp.jsp?arnumber=1626583&tag=1

[18] Comparison of EAPs with Other Actuator Technologies, 2010.
[Accessed online: June 2015] at:
http://ndeaa.jpl.nasa.gov/nasa-nde/lommas/eap/actuators-comp.pdf

[19] T W Duerig, K N Melton, D Stöckel, Engineering Aspects of Shape Memory Alloys, 1990, pages 3-21, 234-244.

[20] T. Matsunaga et al., Tactile display using shape memory alloy micro-coil actuator and magnetic latch mechanism, 2013, [Accessed online: June 2015] at: http://www.sciencedirect.com/science/article/pii/S0141938213000243

[21] Brad H., Dava N., Low spring index, large displacement shape memory alloy (SMA) coil actuators for use in macro- and micro-systems, 2014, [Accessed online: June 2015] at: proceedings.spiedigitallibrary.org/proceeding.aspx?doi=10.1117/12.2044406

[22] Luo, Y. et al., A Shape Memory Alloy Actuator Using Peltier Modules and R-Phase Transition Journal of Intelligent Material Systems and Structures, July 2000 vol. 11 no. 7503-511, [Accessed online: June 2015] at: http://jim.sagepub.com/content/11/7/503.full.pdf+html

[23] Berguer R. et al., An ergonomic comparison of in-line vs pistol-grip handle configuration in a laparoscopic grasper, Surg Endosc., 1998, Jun;12(6):805-8 [Accessed online: June 2015] at: http://link.springer-ny.com/link/service/journals/00464/bibs/12n6p805.html

[24] Mucksavage, P. et al., Differences in grip forces among various robotic instruments and da Vinci surgical platforms, JOURNAL OF ENDOUROLOGY Volume 25, Number 3, March 2011 p. 523–528., [Accessed online: June 2015] at:http://online.liebertpub.com/doi/pdf/10.1089/end.2010.0306

[25] Westebring-Van Der P. et al., Effect of laparoscopic grasper force transmission ratio on grasp control, Surg Endosc (2009) 23:818–824, [Accessed online: June 2015] at: http://download.springer.com/

[26] Ali Faraz, Shahram Payandeh, Engineering Approaches to Mechanical and Robotic Design for Minimally Invasive Surgeries, 2000, p.58.

[27] Richard G. Budynas, J. Keith Nisbett, Shingley's Mechanical Engineering Design, 2007, p. 400, 625.

[28] Technical Characteristics of FLEXINOL® Actuator Wires, [Accessed online: June 2015] at: http://www.dynalloy.com/pdfs/TCF1140.pdf

[29] Maxon flat series motor specification, part 301999, [Accessed online: June 2015] at: http://www.maxonmotor.com/medias/sys_master/root/8816806133790/15-251-EN.pdf

[30] FSR-149AS IEEm pressure sensor specification, International Electronics Engineering, [Accessed online: June 2015] at: http://www.soselectronic.com/a_info/resource/c/FRS_pressure_sensors.pdf